

# Miocene to Pleistocene sporomorphs and dinoflagellates from plankton-dated sediments in the NDO B-1 well, offshore Nile Delta, Egypt

MAGDY S. MAHMOUD\*, MENNAT-ALLAH T. EL HUSSIENY and AMR S. DEAF

Geology Department, Faculty of Science, Assiut University, Assiut 71516, Egypt

\* Corresponding author: magdysm@aun.edu.eg

## ABSTRACT:

Mahmoud, M.S., El Hussieny, M.-A.T. and Deaf, A.S. 2025. Miocene to Pleistocene sporomorphs and dinoflagellates from plankton-dated sediments in the NDO B-1 well, offshore Nile Delta, Egypt. *Acta Geologica Polonica*, **75** (4), e59.

Based on well-preserved palynomorphs a biostratigraphic assessment of the Miocene to Pleistocene succession in the NDO B-1 well, Nile Delta area, Egypt, is presented. Terrestrial pollen and spores are relatively more abundant and diverse in their spectra than the marine dinoflagellate cysts, which has enabled their semi-quantitative estimation. Dinoflagellate cysts are investigated on a qualitative basis. Two informal spore-pollen zones and seven informal zones based on dinoflagellate cysts are suggested and calibrated by planktonic foraminifera and calcareous nannoplankton zones in the well; on a local scale they can be useful in the Nile Delta area. The results were compared with the Cenozoic palynomorph associations in the Mediterranean and Paratethyan realms. The dinoflagellate cyst taxa around the Messinian–Zanclean boundary in the well log lack characteristic brackish Paratethyan taxa, which is probably due to a disconnection or limited water circulation between the Paratethys and the eastern Mediterranean at the Messinian–Zanclean boundary or related to a stratigraphic bias.

**Key words:** Spores; Pollen; Dinoflagellate cysts; Zonation; Paleobiogeography; Eastern Mediterranean.

## INTRODUCTION

The Neogene is a period of interest in the geological history of the Mediterranean and Paratethys areas due to significant tectonic, climatic and environmental settings. The Tethys witnessed a major fragmentation in the Cenozoic and, subsequently, the Paratethys became isolated, and the Mediterranean Basin evolved. This isolation resulted in distinct fossil assemblages of brackish or freshwater nature, as documented by, e.g., dinoflagellate cysts, which reflect a significantly reduced biodiversity during the Messinian Salinity Crisis (MSC) events (5.97–5.33 Ma) in the Mediterranean area (e.g., Hsü *et al.* 1973; Roveri *et al.* 2008), with intense subaerial erosion of the basin margins (e.g., Clauzon *et al.* 1996).

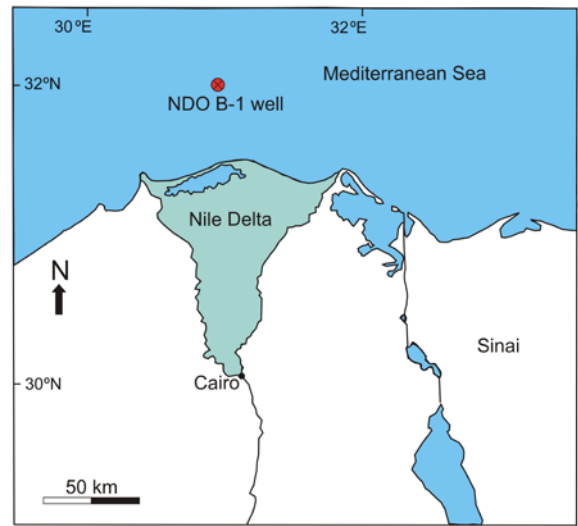
Few palynological works have so far been published on the Cenozoic sedimentary succession of the Egyptian Nile Delta and in the nearby Gulf of Suez area. El Beialy (1988) studied Neogene subsurface rocks from the Kafr El-Dawar well no. 1 and recognized six, lower Oligocene to Pliocene, dinoflagellate assemblage zones (A to F), correlated on a local and global scale. El-Beialy (1997) studied the content of miospores and dinoflagellate cysts across the Miocene–Pliocene boundary in the Kafr El Sheikh-1 well in the northern Nile Delta, dating the El Wastani and Kafr El Sheikh formations to the Early Pliocene, underlain by the Abu Madi Formation (Upper Miocene), based on the presence of the dinoflagellate cysts *Dapsilidinium pseudocollegerum* (Stover) Bujak, Downie and Williams,



© 2025 Magdy S. Mahmoud, Mennat-Allah T. El Hussieny and Amr S. Deaf. This is an open access article under the CC BY license (<http://creativecommons.org/licenses/by/4.0/>), which permits use, distribution, and reproduction in any medium, provided that the article is properly cited.

1980, *Hystrichosphaeropsis obscura* Habib, 1972 and *Selenopemphix dionaeacysta* Head, Norris and Mudie, 1989a. The Miocene–Pliocene boundary was regarded to have been situated between the uppermost part of the Abu Madi Formation and the lowermost part of the Kafr El Sheikh Formation (El-Beialy 1992). Mahmoud (1993) investigated some core samples from the Kareem Formation, penetrated by the Shagar-1 well, southwest of the Gulf of Suez and suggested two informal dinoflagellate cyst assemblages (zones A and B). Accordingly, the overlapping occurrence of *Systematophora placacantha* [now *Cleistosphaeridium placacanthum* (Deflandre and Cookson) Eaton, Fensome, Riding and Williams, 2001] and *Hystrichosphaeropsis obscura* was supposed to correlate with the Middle Miocene. Soliman *et al.* (2012) carried out a palynological investigation on the Lower to Middle Miocene deposits of the Gulf of Suez and established five dinoflagellate cyst zones, with a *Polysphaeridium zoharyi* Assemblage Biozone (GOS5; upper Langhian and Serravallian?). El Atfy *et al.* (2017) carried out a palynological investigation of the Miocene Rudeis and Kareem formations (Gharandal Group), in the GH 404-2A well, Gulf of Suez, Egypt. They established one sporomorph and three dinoflagellate cyst zones, and highlighted the importance of dinoflagellate cysts as good biostratigraphic correlation tools in the Miocene of the Gulf of Suez, the Nile Delta and northern Sinai. El-Soughier and Mahmoud (2019) studied the palynological content of some Neogene sediments (Miocene) penetrated by the GS9-1X well in the northern Gulf of Suez, Egypt. They dated the interval to the Lower Miocene according to the presence of the dinoflagellate cysts *Exochosphaeridium insigne* de Verteuil and Norris, 1996, *Sumatradinium soucouyantiae* de Verteuil and Norris, 1992 and *Hytrichokolpoma rigaudiae* Deflandre and Cookson, 1955.

In this work, we present a Neogene–Quaternary record of organic-walled microfossils (mainly pollen, spores and dinoflagellate cysts) from the NDO B-1 well (Text-fig. 1). We focus on the composition, diversity and abundance of terrestrial pollen and spores. Dinoflagellate cysts proved to be relatively less diverse than the miospores. Therefore, they were treated on a qualitative (presence/absence) basis. An (informal) palynomorph zonation is attempted, which can be applied on a regional scale in the Nile Delta area. Such a zonation can be robust due to the presence of an independent age control (planktonic foraminifera and calcareous nannoplankton) in the well under investigation. The work aims also at comparing the current palynological data to those in



Text-fig. 1. Map showing the location of the NDO B-1 well, offshore Nile Delta, Egypt.

other parts of the Mediterranean and the Paratethys. The interval occupied by the MSC events (Qawasim and Rosetta formations) is spanned at length in the well. Independent dating based on planktonic foraminifera (Ouda and Obaidalla 1995; Makled *et al.* 2017) and calcareous nannoplankton (Makled and Mandur 2016; Mandur and Makled 2016) is available from previous studies of the well, where the presumed MSC interval has been regarded as nonfossiliferous. The recovered palynomorphs are therefore needed to offer insights into these events. In this context, the recovered dinoflagellate cysts serve as indicators inferring the relationship between the Mediterranean and the Paratethys realms during the Neogene.

## GEOLOGICAL SETTING

The Nile Delta area has been considered part of the colliding African Plate along the southern shores of the Mediterranean Sea (Harms and Wary 1990). It occupies an area of approximately 22,000 km<sup>2</sup> situated in the northeastern margin of the African Plate and is considered one of the earliest known deltas in the world. The area was part of the Tethys Ocean during the Late Cretaceous. Tectonics in the area influenced the facies distribution due to the formation of several paleo-highs and lows. Continuous subsidence resulted in a thick Neogene succession in the North Nile Delta Basin (Sestini 1995). Six major structural trends delineate the present Nile Delta and affect the

distribution of its Miocene sediments (Abdel Aal *et al.* 1994). The deltaic sequence of the Nile Delta consists of two clastic units, separated by an unconformity surface (see Shalaby and Sarhan 2023).

The regional geology of the Nile Delta area has been extensively studied (e.g., Rizzini *et al.* 1978; Barber 1981; Sestini, 1989; Hamouda and El-Gharabawy 2019; Metwalli *et al.* 2023; Shalaby and Sarhan 2023). Regional lithological and geo-physical correlation of these units is not easy due to lack of sharp vertical facies changes, since they are made up mainly of siliciclastics (see Farouk *et al.* 2014; Metwalli *et al.* 2023). Therefore, the designation and usage of rock units in the Neogene–Quaternary section of the Nile Delta area is in part controversial, particularly at the Miocene–Pliocene transition, due to its regional widespread unconformable nature. Consequently, the term Abu Madi (Pliocene) Formation is sometimes applied as an equivalent to the Qawasim (Miocene) Formation, or as a Miocene rock unit overlying the Qawasim Formation. However, according to the most acceptable and widely-used lithostratigraphic classification of Rizzini *et al.* (1978), the clastic sedimentation of the area consists of a Miocene cycle, which is subdivided into the Sidi Salem, Qawasim, and Rosetta formations, a Pliocene–Quaternary cycle, which consists of the Abu Madi, Kafr El-Sheikh, El Wastani and Mit Ghamr formations, and a Holocene cycle (Bilqas Formation).

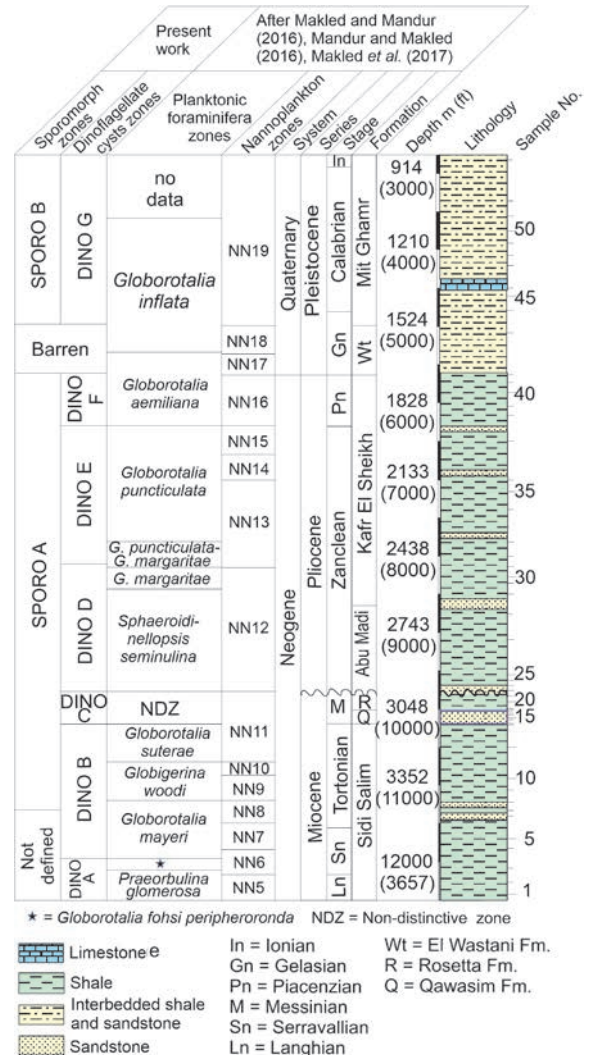
## LITHOSTRATIGRAPHY

The Neogene–Quaternary rock succession in the NDO B-1 well (Text-fig. 2) is subdivided according to stratigraphic information presented in N.C.G.S. (1976), Rizzini *et al.* (1978), E.G.P.C. (1994) and Makled *et al.* (2017). The rock formations of this time interval in the Nile Delta area are briefly summarized, from base to top, in the following paragraphs. For additional information the reader is kindly referred to Mahmoud *et al.* (2024) and El Hussieny *et al.* (2025).

### Sidi Salim Formation

**Age:** Middle to Late Miocene (Langhian to Tortonian) (Rizzini *et al.* 1978; Abdel-Kireem *et al.* 1984; Abdou *et al.* 1984; Ismail *et al.* 2010; Mandur and Makled 2016; Makled *et al.* 2017).

**Lithology:** This rock unit is composed of clay with a few intervals of dolomitic marl, sandstone and siltstone interbeds. It is about 446 m thick in its type-sec-



tion in the Sidi Salim-1 well (Rizzini *et al.* 1978). In the NDO B-1 well, its thickness is about 213 m, the base is not recognizable, and the top is traced below the sandy and conglomeratic beds of the overlying Qawasim Formation. Toward the southern delta it probably lies on the Moghra Formation or older rock units. In the offshore area, this rock unit is overlain by the Messinian Qawasim clastics and Rosetta anhydrites, or by the Pliocene clays of the Abu Madi and Kafr El Sheikh formations.

## Qawasim Formation

*Age:* Late Miocene (Messinian) (Rizzini *et al.* 1978; Barber 1981; Makled *et al.* 2017).

*Lithology:* The formation consists of sand pebbles, sandstones and conglomerates (Rizzini *et al.* 1978), with a lenticular shape and slump structures. The type-section of the formation is in the Qawasim-1 well (~ 933 m thick). In the offshore NDO B-1 well, the formation thins out to about 60 m of sandstones. At the base, the coarser sandy layers display erosional features. The conglomerates are generally massive and may show planar cross-bedding. Frequently there occur layers of peat and coal fragments. The upper limit of this unit is difficult to define on the basis of subsurface data alone (Rizzini *et al.* 1978).

## Rosetta Formation

*Age:* Late Miocene (Messinian) (Rizzini *et al.* 1978; Barber 1981; Makled *et al.* 2017).

*Lithology:* The formation (~40 m thick in the Rosetta no. 2 type well) is composed of anhydrite interbedded with thin clay beds (Rizzini *et al.* 1978), which are barren of fossils. The unit is completely missing in the southern onshore parts of the delta, while in the north offshore areas it terminates below Lower Pliocene marine clays. The formation can be correlated with the Messinian evaporites of the Mediterranean Basin (Barber 1981). The Qawasim and Rosetta formations terminate the Miocene cycle in the Nile Delta area; they accumulated during the MSC events, with a very low fossil content and a marked hiatus in the Nile Delta area (e.g., Cherif *et al.* 1993), as in other regions of the Mediterranean (e.g., Iaccarino and Salvatori 1982). In the NDO B-1 well, the Rosetta Formation is about 38 m thick.

## Abu Madi Formation

*Age:* Early Pliocene (Zanclean) (Rizzini *et al.* 1978; Abdel-Kireem *et al.* 1984; Abdou *et al.* 1984; Ismail *et al.* 2010; Makled and Mandur 2016; Makled *et al.* 2017).

*Lithology:* The formation consists of thick sand and clay interbeds (321 m in the Abu Madi no. 1 type well) (Rizzini *et al.* 1978), with fauna-lacking conglomerates in the basal parts. The sands show large-scale cross-bedding while bioturbation is common in the clays. Foraminifera are frequent in the clay intervals and are typical for the Lower Pliocene of the Mediterranean Sea area (Cita 1973). As can be seen

from Makled *et al.* (2017) in the NDO B-1 borehole, the base of the Abu Madi Formation was traced in the top of the Non-distinctive zone (NDZ), which is equivalent to the Qawasim and Rosetta formations. The NDZ was originally defined by Iaccarino and Salvatori (1982); its base was dated at 5.96 Ma, while its top ends at 5.332 Ma (Lourens *et al.* 2004). Rizzini *et al.* (1978) stated that the Abu Madi Formation lies on a fairly pronounced erosion surface. In the NDO-B1 well, it is represented by 176 m of sand and clay interbeds. The formation was deposited during the Messinian but was reworked during the Early Pliocene transgression (Sestini 1989). In the onshore Nile Delta the formation reflects a progressive drowning of an incised valley, bounded at the base by an erosional unconformity, created by the late Messinian sea-level drop, and at the top by a drowning unconformity related to the Early Pliocene transgression (Metwalli *et al.* 2023).

## Kafr El Sheikh Formation

*Age:* Pliocene (Zanclean–Piacenzian) (Rizzini *et al.* 1978; Abdel-Kireem *et al.* 1984; Abdou *et al.* 1984; Ismail *et al.* 2010; Makled and Mandur 2016; Makled *et al.* 2017). The age of this formation is easily defined due to the presence of the Lower Pliocene *Globorotalia margaritae* and *Globorotalia puncticulata* zones and the Middle Pliocene *Globorotalia aemiliana* and *Globorotalia crassaformis* zones (Rizzini *et al.* 1978).

*Lithology:* The type-section, about 1458 m thick, is the Kafr El Sheikh well no. 1. This fairly thick unit is widespread over the whole delta area and consists of clay and sand interbeds. In the NDO B-1 well, it comprises clays with a few sand beds, 1088 m thick. The clays consist of kaolinite and montmorillonite with a minor admixture of illite (Rizzini *et al.* 1978).

## El Wastani Formation

*Age:* Pleistocene (Gelasian) (Makled and Mandur 2016; Makled *et al.* 2016).

*Lithology:* The type-section of this formation, about 123 m thick, is the El Wastani well no. 1. The formation consists of thick sands interbedded with thin clays, which become thinner towards the top of the unit. Sands are quartzose, coarse to medium grained, while clays are soft and very sandy. The upper limit of the El Wastani Formation is uncertain due to the gradual decrease in clay thickness (Rizzini *et al.* 1978). In the NDOB-1 well, the formation is about 167 m thick.

## Mit Ghamr Formation

**Age:** Pleistocene (Gelasian–Calabrian) (Makled and Mandur 2016; Makled *et al.* 2017).

**Lithology:** The type-section of this formation, about 463 m thick, is the Mit Ghamr well no.1. It consists of thick layers of sand and pebbles that contain clay interbeds. The sands are quartzose, medium to coarse-grained while the pebbles consist of quartzite, chert and dolomite. This rock unit reflects the filling of the basin by coastal sands or Nile deposits (Rizzini *et al.* 1978). In the NDOB-1 well, the formation measures about 481 m.

## MATERIAL AND METHODS

The present work deals with the palynostratigraphy of the Neogene–Quaternary succession in the NDO B-1 well (32°05'57"N 30°53'16"E). The well was drilled by ESSO in 1975 in the offshore Nile Delta (eastern Mediterranean). Fifty-three cuttings samples were used in this study (see Text-fig. 2), of which forty-five were considered suitable for biostratigraphic analysis. Samples were digested by HCl (35%) and HF (40%) following the standard palynological processing techniques (e.g., Traverse 2007) to remove carbonates and silicates, respectively. Residues were sieved through a 15 µm mesh after mild ultrasonic treatments to concentrate palynomorphs and eliminate unwanted material (e.g., amorphous organic matter). Permanent slides were prepared using glycerin jelly as the mounting medium for light microscopy. Slides were examined using a Leica DM LB2 light microscope equipped with a Leica DFC 280 digital camera at the Geology Department of Assiut University, Egypt.

At least, seven slides were counted (glass cover slip 20×20 mm and 45×25 mm across) to account for the semi-quantitative estimate of the sporomorph associations. Additional slides were scanned for qualitative purposes. A count of more than 200 palynomorphs (spores, pollen, dinoflagellate cysts and other miscellaneous components such as freshwater algae and microforaminiferal linings) was established for the majority of the samples (see Appendix). Spores and pollen were found to be more abundant compared to the dinoflagellate cysts. For this reason, their semi-quantitative percentage frequencies were calculated. Dinoflagellate cysts are highly diluted due to the terrestrial influx of the Nile River (i.e., both sporomorphs and freshwater algae) and were, therefore, investigated on a qualitative (presence/absence) basis. The slides

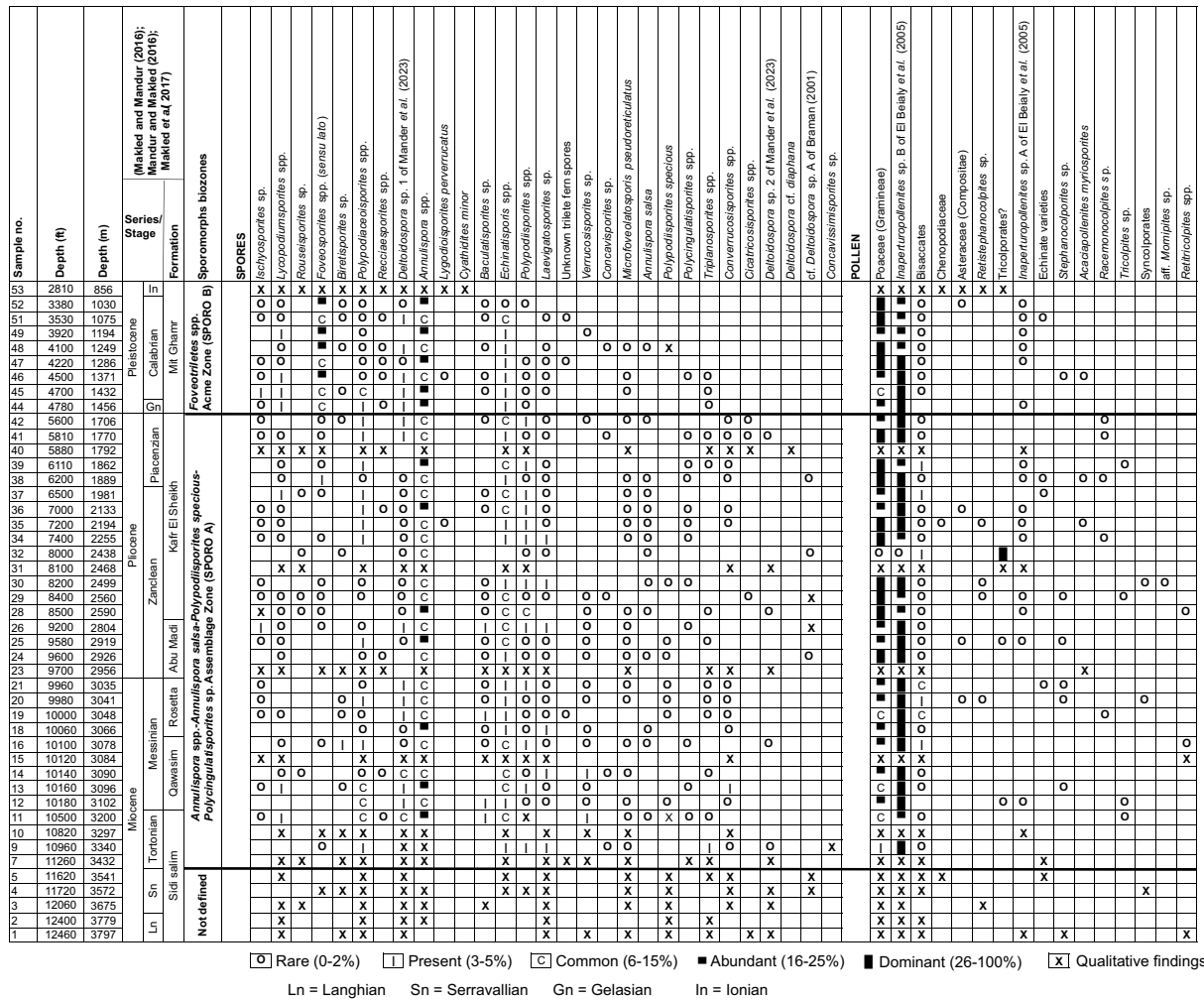
and residues are housed in the Geology Department, Faculty of Science, Assiut University, Egypt.

## PALYNOLOGICAL RESULTS

Palynomorph associations from the NDO B-1 well section contain terrestrial (spores, pollen, freshwater algae) and marine (dinoflagellate cysts, microforaminiferal linings) organic-walled microfossils. In general, the preservation of palynomorphs was moderate to good. Freshwater algae were the main contributors of the palynomorphs (up to 60% of total palynomorphs). The majority of the samples contain abundant terrestrial spores and pollen (sometimes reaching over 90% of the total palynomorphs) while the dinoflagellate cysts were relatively less abundant. Only in a single horizon did these dinocysts reach more than 80% of the total palynomorphs. For a detailed description of the total palynofacies content in the NDO B-1 well please refer to Mahmoud *et al.* (2024). Twenty-nine genera of spores and pollen, in addition to bisaccates, representatives of the families Chenopodiaceae, Asteraceae (Compositae) and Poaceae (Gramineae), along with other pollen, were documented in the Neogene–Quaternary succession of the well. Dinoflagellate cysts, although less abundant than spores and pollen, are relatively more diverse, documented by twenty genera and more than forty species. The lowest diversities were observed in a few samples (Qawasim Formation, sample 15, 3084 m; Rosetta Formation, sample 18, 3066 m; Kafr El Sheikh Formation, sample 32, 2438 m; Mit Ghamr Formation, sample 44, 1456 m). We did not observe a lack of dinoflagellate cysts at the Miocene–Pliocene (Messinian–Zanclean) transition (Qawasim/Rosetta and basal Abu Madi formations), in contrast to the extinction of planktonic foraminifera in the same interval. All palynomorphs identified in this study and their stratigraphic distribution are presented in two distribution charts (Text-figs 3 and 4) and illustrated in Text-figs 5 to 10.

## PALYNOLOGICAL BIOZONATION

Two informal spore-pollen zones and seven informal zones based on dinoflagellate cysts are proposed herein. These zones are believed to reflect a localized/restricted nature in the Nile Delta palynomorph spectrum, whose species diversity and abundance was highly impacted by the Nile influx during the Neogene–Quaternary. In such conditions, establishing a zonation scheme based on the non-contin-



Text-fig. 3. Semi-quantitative distribution chart of spores and pollen, by highest occurrence, in the NDO B-1 well, showing the proposed spore-pollen zones (based on data counts presented in the Appendix).

uous occurrences, coupled with the presence of numerous long-ranging species, requires a correlation with another prominent environmental, stratigraphic or other recognizable geologic phenomenon. In this context, events such as palynofloral peaks, unconformity surfaces, and, as previously suggested, palynologically-based, sequence stratigraphic boundaries (Mahmoud *et al.* 2024) were incorporated to make the palynological zonation more robust. It is worth noting here that the section investigated is not characterized by a wide range of vertical environmental changes from e.g., terrestrial to marine. This can result in the lack of many facies-controlled taxa, such as outer shelf/oceanic dinoflagellates, which prevents a more comprehensive description of the zones. Both the uppermost (UO) and the lowest (LO) occurrences

of species are used to delineate these zones. The investigated Miocene–Pleistocene succession of the NDO B-1 well has been independently dated by planktonic foraminifera (Makled *et al.* 2017, pp. 476–480) and calcareous nannoplankton (Mandur and Makled 2016, Miocene, pp. 7–12; Makled and Mandur 2016, Pliocene–Pleistocene, pp. 380–382). For detailed information on these plankton zones and their recognition and calibration with the standard refer to these publications..

## Sporomorph zones

### SPORO A Assemblage Zone

**Age:** Late Miocene to Pliocene (Tortonian to Piacenzian).

Sample no.	Depth (ft)		Depth (m)		Series/Stage		(Makled and Mandur 2016; Mandur and Makled 2016; Makled et al. 2017)	
	Depth (ft)	Depth (m)	Formation	Formation				
53	2810	856			In		Dinoflagellate cysts biocores (informal)	
52	3380	1030					<i>Seleropempix quanta</i>	
51	3530	1075					<i>Operculodinium centrotcarban</i>	
49	3920	1194					<i>Spiniferites ramosus</i>	
48	4100	1249					<i>Polysphaeridium zoharyi</i>	
47	4220	1286					<i>Operculodinium israelanicum</i>	
46	4500	1371					<i>Spiniferites cf. delicatus</i>	
45	4700	1432					<i>Hystriechokolpoma spp.</i>	
44	4780	1456					<i>Spiniferites cf. bullidoicus</i>	
42	5600	1706					<i>Echinidinium spp.</i>	
41	5810	1770					<i>Lejeuneacysta spp.</i>	
40	5880	1792					<i>Spiniferites mirabilis</i>	
39	6110	1862					<i>Cymatiosphaera sp.</i>	
38	6200	1889					<i>Impagidinium patulum</i>	
37	6500	1981					<i>Hystriechokolpoma rigidae</i>	
36	7000	2133					<i>Spiniferites cf. pacificus</i>	
35	7200	2194					<i>Spiniferites pachydarmus</i>	
34	7400	2255					<i>Tectatodinium pellitum</i>	
32	8000	2438					<i>Impagidinium spp.</i>	
31	8100	2468					<i>Spiniferites cf. multisphaerus</i>	
30	8200	2499					<i>Systematophora spp.</i>	
29	8400	2560					<i>Spiniferites hainanensis</i>	
28	8500	2590					<i>Membranilirnacia? sp.</i>	
26	9200	2804					<i>Melitisphaeridium sp.</i>	
25	9580	2919					<i>Nematosphaeropsis labyrinthus</i>	
24	9600	2926					<i>Seleropempix nephrodes</i>	
23	9700	2956					<i>Achromosphaera sp.</i>	
21	9960	3035					<i>Brigantedinium spp.</i>	
20	9980	3041					<i>Homotrylillum spp.</i>	
19	10000	3048					<i>Impagidinium cf. patulum</i>	
18	10060	3066					<i>Seleropempix brevispinosa</i>	
16	10100	3078					<i>Impagidinium paradoxum</i>	
15	10120	3084					<i>Polykrikos schwarzii</i>	
14	10140	3090					<i>Voradinium spinosum</i>	
13	10160	3096					<i>Pentapharsodinium dalei</i>	
12	10180	3102					<i>Spiniferites twistrigiansis</i>	
11	10500	3200					<i>Homotrylillum acutatum</i>	
10	10820	3297					<i>Homotrylillum tenuispinosum</i>	
9	10960	3340						
7	11260	3432						
5	11620	3541						
4	11720	3572						
3	12060	3675						
2	12400	3779						
1	12460	3797						

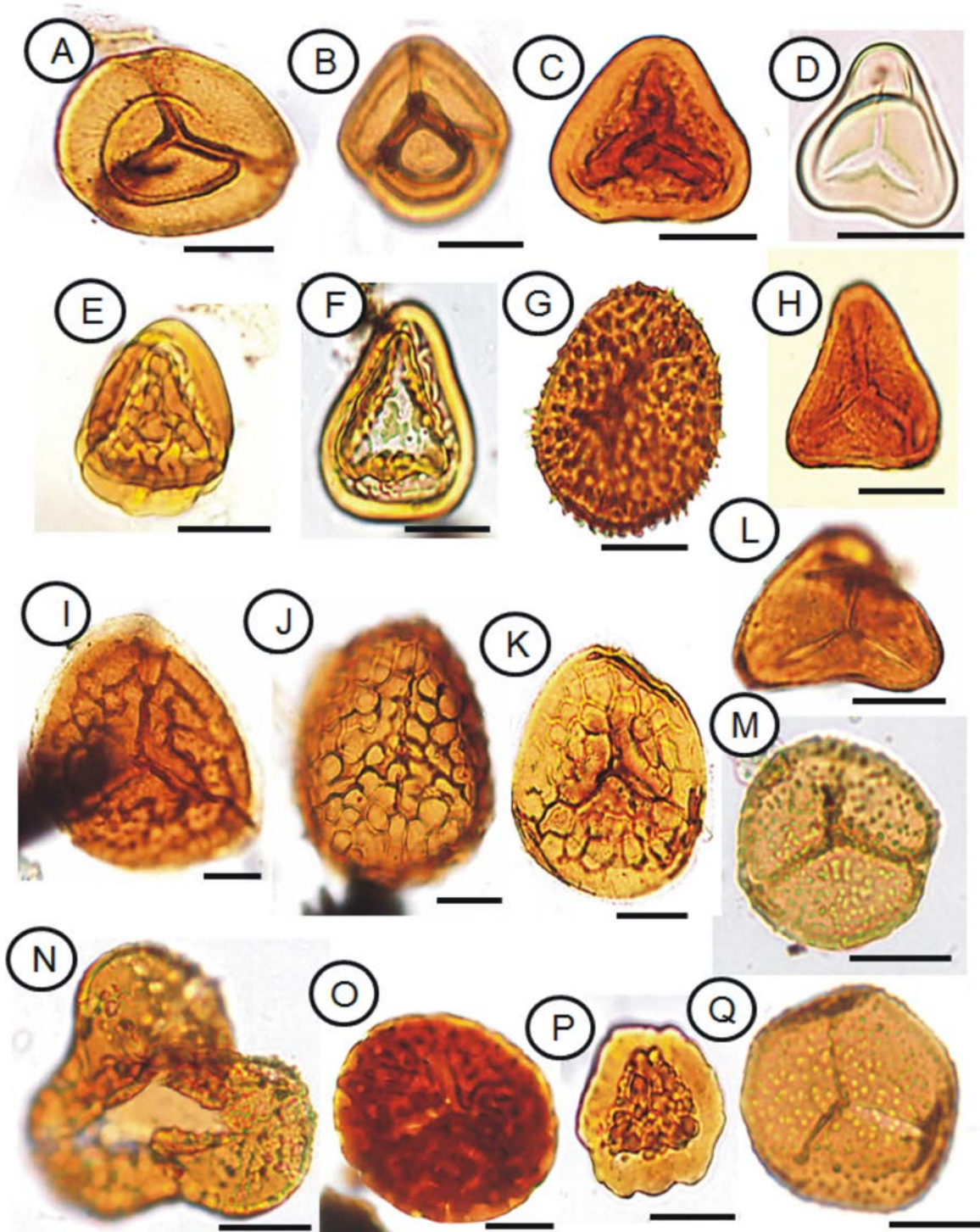
Ln = Langhian    Sn = Serravallian    Gn = Gelasian    In = Ionian

Text-fig. 4. Distribution chart (presence/absence), by highest occurrence, in the NDO B-1 well, showing the proposed dinoflagellate cyst zones (based on data presented in the Appendix).

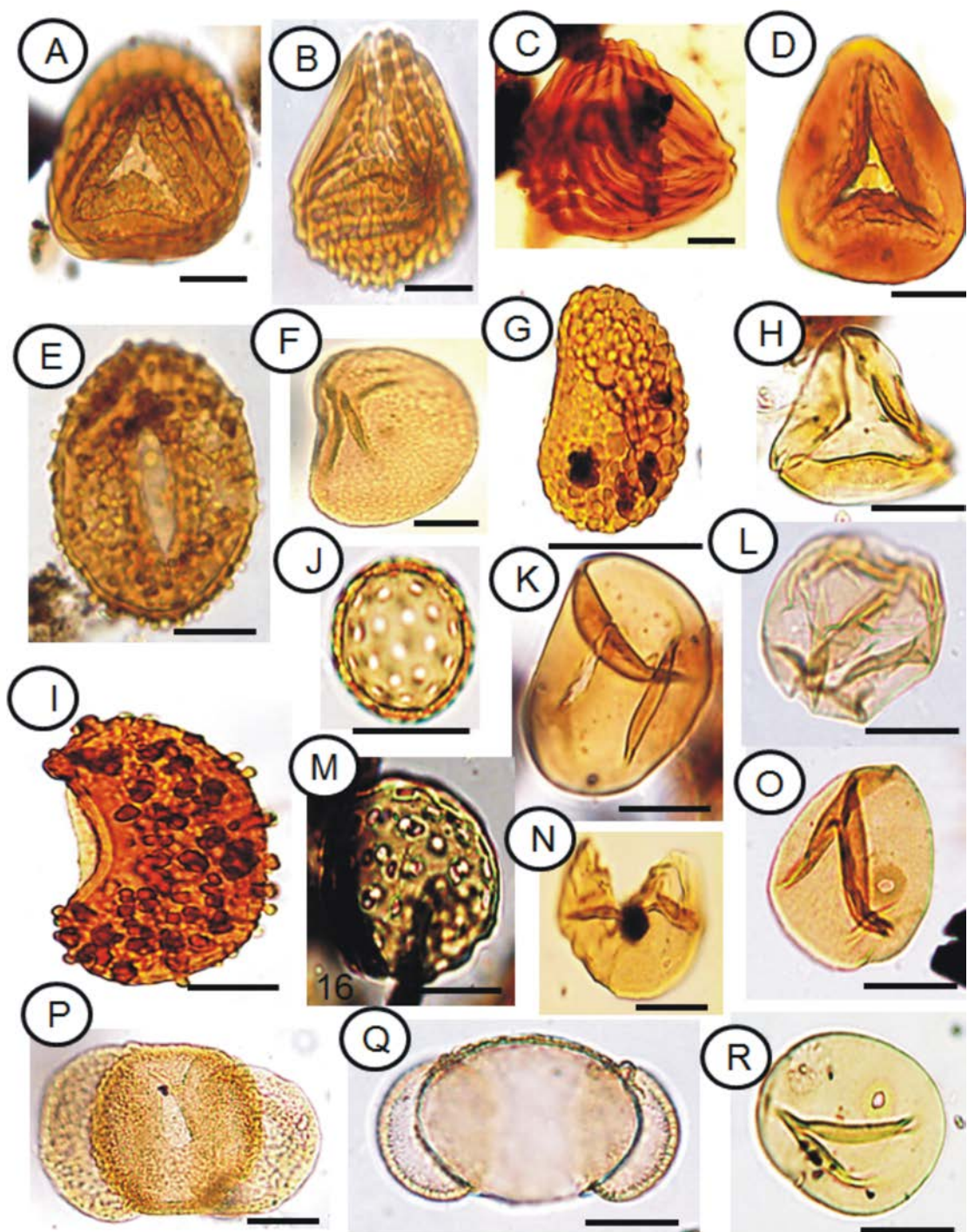
**Lithostratigraphic units:** Upper Sidi Salim, Qawasim, Rosetta, Abu Madi and Kafr El Sheikh formations.

**Paleoenvironment:** Coastal to inner neritic in the Qawasim, Rosetta, Abu Madi and lower Kafr El Sheikh formations; neritic in the upper Sidi Salim and uppermost Kafr El Sheikh formations (Mahmoud *et al.* 2024).

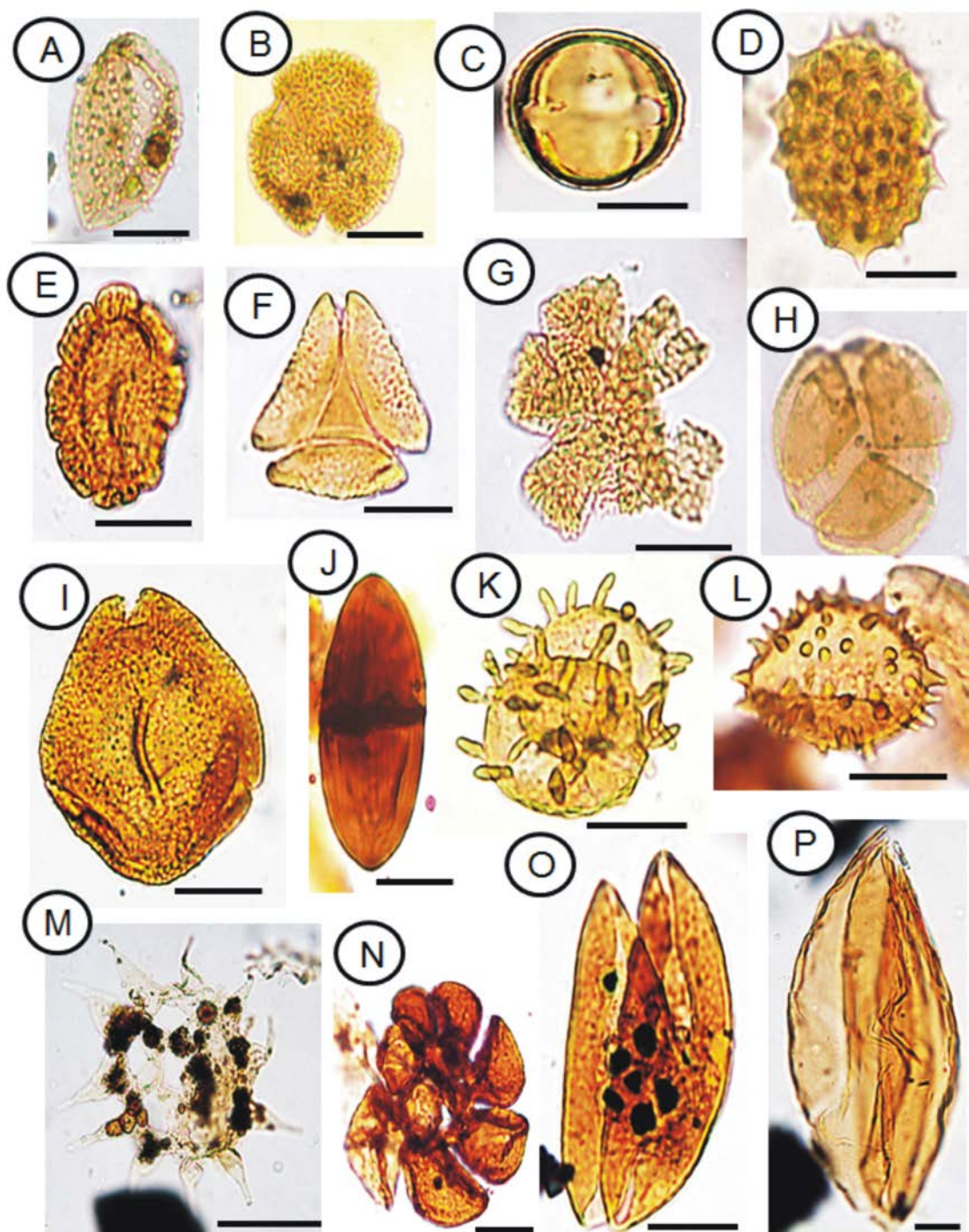
**Calibration:** Planktonic foraminifera – from the top part of the *Globorotalia mayeri* Interval Zone to the top part of the *Globorotalia aemiliana* Interval Zone (see dinoflagellate cyst zone description in this work for equivalent standard planktonic zones); Nannoplankton – zones NN8 to NN16, Tortonian to Piacenzian (Miocene–Pliocene) (after Mandur and Makled 2016; Makled and Mandur 2016).



Text-fig. 5. Pollen and spores in the NDO B-1 well. A – *Annulispera salsa* Braman, 2001; a (37), 1981 m, 37/97.5. B – *Polycingulatisporites* sp., d (39), 1862 m, 48.1/112.6. C, E, F – *Polypodiaceoisporites* spp.; C – d (25), 2919 m, 38.2/99; E – d (25), 2919 m, 31/98.6; F – a (44), 1456 m, 44.8/97.1. D – *Cyathidites minor* Couper, 1953, g (53), 856 m, 36.8/106.8. G – *Echinatisporis* sp., a (51), 1075 m, 41.7/106.9. H – *Deltoidospora* sp. 1 of Mander et al. (2023), q (26), 2804 m, 27.2/99.8. I, J – *Recciaesporites* sp.; I – b (40), 1792 m, 53.6/103.5; J – a (48), 1249 m, 38.7/114.4. K – *Rouseisporites* sp., d (37), 1981 m, 39.5/98.1. L – *Deltoidospora* sp. 2 of Mander et al. (2023), c (41), 1770 m, 35.7/113.1. M, Q – *Foveosporites* sp. (*sensu lato*); M – a (44), 1456 m, 51.7/98.8; Q – b (51), 1075 m, 49/104. N – *Convavissimisporites* sp., c (9), 3340 m, 55.5/110. O – *Ischyosporites* sp., b (47), 1286 m, 41.2/93.7. P – aff. *Polypodiaceoisporites* sp., c (25), 2919 m, 33/109. Slide symbols, sample numbers (in brackets), depths and microscope co-ordinates are given for every illustrated specimen. Scale bar = 20  $\mu$ m.



Text-fig. 6. Pollen and spores in the NDO B-1 well. A–C – *Cicatricosisporites* sp.; A – b (40), 1792 m, 52.5/94.7; B – b (28), 2590 m, 33.7/94.3; C – k (1), 3797 m, 39.6/115.3 (?reworked). D – *Polypodiaceoisporites* sp., n (4), 3572 m, 32.3/110. E, I – *Polypodiisporites* sp.; E – b (47), 1286 m, 19.3/98.7; I – d (39), 1862 m 38.6/105 (with baculate ornament). F – *Microfoveolatiosporis pseudoreticulatus* (Hedlund) Singh, 1983, a (14), 3090 m, 34/110.2. G – *Polypodiisporites speciosus* Sah, 1967 *sensu* Mander *et al.* (2023), 1 (3), 3675 m, 34.7/106.9. H – cf. *Deltoidospora* sp. A of Braman (2001), n (5), 3541 m, 50/93.3. J, M – Chenopodiaceae pollen; J – m (53), 856 m, coordinates lost; M – n (5), 3541 m, 50.7/96.9. K – *Laevigatosporites* sp., d (29), 2560 m, 38.2/109.6. L – *Inaperturopollenites* sp. B of El Beialy *et al.* (2005), b (31), 2468 m, 47.7/92.8. N – *Inaperturopollenites* sp. A of El Beialy *et al.* (2005), d (29), 2560 m, 24.5/98.6. O, R – Poaceae (= Gramineae) pollen; O – c (39), 1862 m, 46.5/95.8; R – c (52), 1030 m, 40.5/108.5. P, Q – Bisaccate pollen; P – b (39), 1862 m, 49/98.1; Q – b (37), 1981 m, 30/102.1. Slide symbols, sample numbers (in brackets), depths and microscope co-ordinates are given for every illustrated specimen. Scale bar = 20  $\mu$ m.



Text-fig. 7. Pollen and spores (A–L), freshwater algae (M, O, P) and foraminifera test lining (N) in the NDO B-1 well. A – *Racemonocolpites* sp. (cf. *R. facilis* González-Guzmán, 1967), c (41), 1770 m, 41.2/107.7. B – *Retitricolpites* sp., l (3), 3675 m, 37.1/94.3. C – Tricolporate pollen, j (32), 2438 m, 38.6/111.4. D – Asteraceae (Compositae) pollen, b (52), 1030 m, 47/100.6. E – *Stephanocolporites* sp., a (35), 2194 m, 30/104.5. F – Syncolporate angiosperm pollen (finely reticulate variety), d (30), 2499 m, 35.7/111. G – *Retistephanocolpites* sp., c (29), 2560 m, 38/96.8. H – *Tricolpites* sp., c (29), 2560 m, 41.8/109.6. I – *Foveotricolpites giganteus/gigantoreticulatus* group, b (47), 1286 m, 22.1/112.2. J – Fungal spore (*Dicellaesporites* sp.), n (5), 3541 m, 25.6/102.3. K – *Spinizonocolpites baculatus* Muller, 1968, c (12), 3102 m, 40.8/102.3. L – *Spinizonocolpites echinatus* Muller, 1968, a (11), 3200 m, 39.1/103.5. M – *Pediastrum* sp., a (48), 1249 m, 39.2/112.6. N – Planispiral microforaminiferal test lining, a (40), 1792 m, 40.7/100. O, P – *Ovoidites parvus* (Cookson and Dettmann) Nakoman, 1966; O – c (39), 1862 m, 50.3/101.1; P – b (47), 1286 m, 19.5/107. Slide symbols, sample numbers (in brackets), depths and microscope co-ordinates are given for every illustrated specimen. Scale bar = 20  $\mu$ m.

**Definition:** Presence of the spores *Annulispora* spp., *Annulispora salsa* Braman, 2001, *Polypodiisporites* spp., *Cicatricosporites* spp., *Con verrucosporites* spp. and *Deltoidospora* sp. B of Mander *et al.* (2023), and the pollen *Inaperturopollenites* sp. A of El Beialy *et al.* (2005) and *Racemonocolpites* sp.

**Samples:** 7 to 42 (depth interval 3432 to 1706 m).

**Other characteristics:** Pollen of Poaceae and *Inaperturopollenites* spp. are mostly abundant to dominant. Rare occurrences of angiosperm pollen (e.g., tricolpates and tricolporates) were found. The spectra of spores and pollen in this zone have a wide stratigraphic range, which does not allow for a detailed zonal subdivision. The lower part of the zone is characterized by a notable reworking of palynomorphs from older (Cretaceous) material (e.g., *Afropollis jardinus* Doyle, Jardiné and Doerenkamp, 1982 pollen and *Cerodinium granulosum* (Jain and Millepied) Lentin and Williams, 1987, dinoflagellate cyst, after Mahmoud *et al.* 2024).

#### SPORO B Acme Zone

**Age:** Pleistocene (Gelasian–Calabrian to Ionian).

**Lithostratigraphic unit:** Mit Ghamr Formation.

**Paleoenvironment:** Neritic (Mahmoud *et al.* 2024).

**Calibration:** Planktonic foraminifera (excluding samples 51 to 53) – *Globorotalia inflata* Interval Zone (Makled *et al.* 2017), equivalent to standard zone N22 of Blow (1969) and zone MPL6–MPL1 of Cita (1975) (after Makled *et al.* 2017); Nannoplankton – zone NN19 (after Makled and Mandur 2016).

**Remarks:** Makled and Mandur (2016) designated the uppermost interval of the NDO B-1 well as Ionian, which is equivalent to the Chibanian age according to Cohen *et al.* (2013).

**Definition:** Maximum abundance of *Foveosporites* spp.

**Samples:** 44 to 53 (depth interval 1456 to 856 m).

**Other characteristics:** Occurrence of *Annulispora* spp. (common to abundant). *Ischyosporites* sp., *Lycopodiumsporites* spp., *Polypodiaceoisporites* spp., *Baculatisporites* sp., *Echinatisporis* sp., *Polypodiisporites* spp. and *Laevigatosporites* sp. occur regularly in this zone. Pollen of Poaceae (Gramineae) and *Inaperturopollenites* spp. still reflect the same abundance distribution patterns, with fragmentary occurrences of Chenopodiaceae and Asteraceae. Bisaccates occur in the uppermost samples taken from this zone.

#### Dinoflagellate cyst zones

##### DINO A Assemblage Zone

**Age:** Middle Miocene (Langhian–Serravallian).

**Lithostratigraphic unit:** Lower Sidi Salim Formation.

**Paleoenvironment:** Neritic (Mahmoud *et al.* 2024).

**Calibration:** Planktonic foraminifera – *Praeorbulina glomerosa* Interval Zone, equivalent to standard zone N8 of Blow (1969) and *Globorotalia foehsi peripheroranda* Interval Zone of Makled *et al.* (2017), equivalent to standard zones N9 and N10 of Blow (1969) (after Makled *et al.* 2017); Nannoplankton – zones NN5 and NN6 (after Mandur and Makled 2016).

**Definition:** The base of this zone is undefined while its top was delineated below the LO of *Polykrikos schwartzii* Bütschli, 1873 and *Selenopemphix brevispinosa* Head, Norris and Mudie, 1989b.

**Samples:** 1 to 3 (depth interval 3797 to 3675 m).

**Other characteristics:** *Homotryblium tenuispinosum* Davey and Williams, 1966 is restricted to this zone.

*Polysphaeridium zoharyi* (Rossignol) Bujak, Downie, Eaton and Williams, 1980, *Homotryblium* spp., *Lejeuneacysta* spp., *Spiniferites twistringiensis* (Maier) Fensome, Williams, Barss, Freeman and Hill, 1990 and *Cymatiosphaera* sp. occur in this zone. *Lingulodinium machaerophorum* (Deflandre and Cookson) Wall, 1967, *Operculodinium centrocarpum* (Deflandre and Cookson) Wall, 1967, *Selenopemphix quanta* (Bradford) Matsuoka, 1985, *Spiniferites ramosus* (Ehrenberg) Mantell, 1854 and *Spiniferites* spp. are long-ranging taxa, which occur throughout the whole investigated interval (zones DINO A to DINO G). Sporomorphs in this zone are extremely rare, recovered during the qualitative stage of the microscopic work.

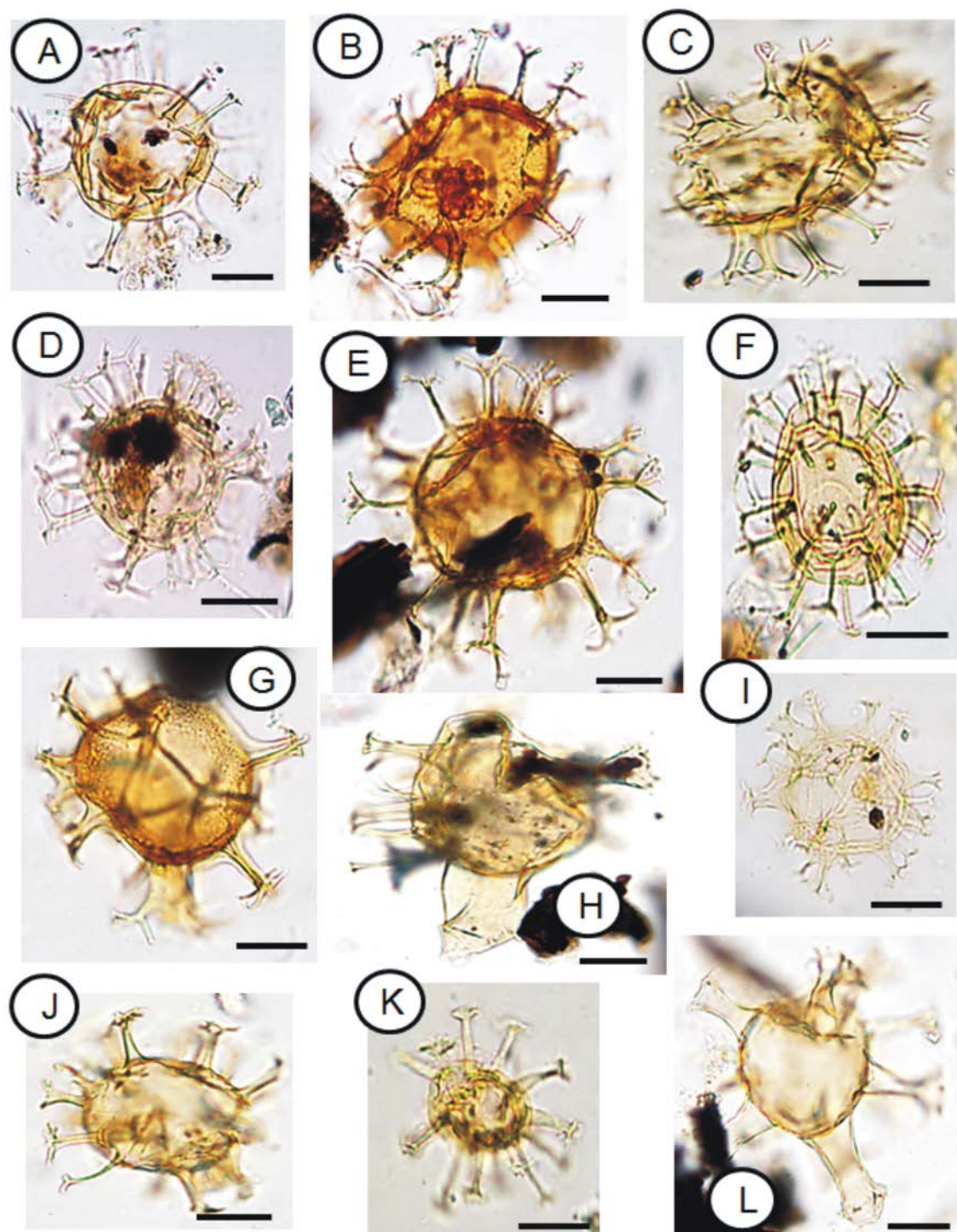
##### DINO B Assemblage Zone

**Age:** Middle–Upper Miocene (Serravallian–Tortonian).

**Lithostratigraphic unit:** Upper Sidi Salim Formation.

**Paleoenvironment:** Neritic (Mahmoud *et al.* 2024).

**Calibration:** Planktonic foraminifera – *Globorotalia mayeri* Interval Zone (Makled *et al.* 2017), equivalent to standard zones N11 to N14 of Blow (1969), *Globigerina woodi* Interval Zone (Makled *et al.* 2017), equivalent to standard zones N15 to N16 of Blow (1969) and the base of the *Globorotalia suterae* Interval Zone (Makled *et al.* 2017), equivalent to standard zone N17 of Blow (1969) (after Makled *et al.* 2017).



Text-fig. 8. Dinoflagellate cysts in the NDO B-1 well. A, J – *Hystrichokolpoma* sp.; A – a (40), 1792 m, 36.5/96; J – c (51), 1075 m, 47.1/110. B – *Spiniferites* cf. *multisphaeratus* Price and Pospelova, 2014, a (40), 1792 m, 37.6/102. C – *Spiniferites* cf. *bulloideus* (Deflandre and Cookson) Sarjeant, 1970, d (52), 1030 m, 41.8/110.2. D – *Spiniferites ramosus* (Ehrenberg) Mantell, 1854, a (40), 1792 m, 55/111.3. E – *Spiniferites hainanensis* Sun and Song, 1992, c (42), 1706 m, 47.8/104.2. F – *Achomosphaera* sp., b (40), 1792 m, 43.6/112.3. G – *Spiniferites pachydermus* (Rossignol) Reid, 1974, b (51), 1075 m, 56.5/108.5. H, L – *Hystrichokolpoma rigaudiæ* Deflandre and Cookson, 1955; H – c (47), 1286 m, 38.3/104; L – b (51), 1075 m, 56.4/106. I – *Spiniferites* cf. *pacificus* Zhao and Morzadec-Kerfourn, 1994, a (51), 1075 m, 45.2/107.7. K – *Melitasphaeridium* sp., a (8), 3414 m, 20/103. Slide symbols, sample numbers (in brackets), depths and microscope co-ordinates are given for every illustrated specimen. Scale bar = 20  $\mu$ m.

al. 2017); Nannoplankton – zones NN7 to NN10 and base of zone NN11 (after Mandur and Makled 2016).

**Definition:** *Selenopemphix brevispinosa*, *Nematosphaeropsis labyrinthus* (Ostenfeld) Reid, 1974, *Polykrikos schwartzii* and *Hystrichokolpoma* sp. first appear in this zone. The top of the zone is delineated below the LO of *Operculodinium israelianum* (Rossignol) Wall, 1967.

**Samples:** 4 to 11 (depth interval 3572 to 3200 m).

**Other characteristics:** *Lejeunecysta* spp., *Spiniferites* cf. *mirabilis* (Rossignol) Sarjeant, 1970, *Melitasphaeridium* sp., *Homotryblium* spp. and *Cymatiosphaera* sp. occur in this zone, whereas *Selenopemphix nephroides* Benedek, 1972 occurs in one sample. Poaceae and Inaperturate pollen are mostly rare, except for samples 9 and 11, where sporomorphs are generally rare.

#### DINO C Assemblage Zone

**Age:** Upper Miocene (Messinian).

**Lithostratigraphic units:** Qawasim and Rosetta formations.

**Paleoenvironment:** Coastal to inner neritic (Mahmoud et al. 2024).

**Calibration:** Makled et al. (2017) assigned this planktonic-barren interval to the Upper Miocene (Messinian) Non-distinctive zone (NDZ), originally defined by Iaccarino and Salvatorini (1982). The base of this zone is dated at 5.96 Ma, and the zone spans an interval from 5.96 to 5.332 Ma (Lourens et al. 2004, orbital tuning).

**Definition:** From the LO of *Operculodinium israelianum* to below the LO of *Impagidinium patulum* (Wall) Stover and Evitt, 1978. *Spiniferites twistringiensis* is restricted to this zone.

**Samples:** 12 to 21 (depth interval 3102 to 3035 m).

**Other characteristics:** *Systematophora* spp. and *Selenopemphix nephroides* occur in this zone. Inaperturate and Poaceae pollen begin their abundance in this zone. In the upper part of the zone, bisaccate pollen becomes common. Representatives of *Annulispora* spores start their abundance one sample below the base of this zone. The top of the zone is bounded by an unconformity surface, which is regionally widespread and well-known in the Nile Delta area (see Shalaby and Sarhan 2023). Within the zone, namely at the base of the Rosetta Formation, the alga *Pediastrum* reaches its acme (Mahmoud et al. 2024).

#### DINO D Interval Zone

**Age:** Pliocene (Zanclean).

**Lithostratigraphic units:** Abu Madi and lower Kafr El Sheikh formations.

**Paleoenvironment:** Coastal to inner neritic (Mahmoud et al. 2024).

**Calibration:** Planktonic foraminifera – *Sphaerodinellopsis seminulina* Acme Zone (Makled et al. 2017), equivalent to the middle part of the standard zone N18 of Blow (1969) and zone MLP1 of Cita (1975), the *Globorotalia margaritae* Interval Zone (Makled et al. 2017), equivalent to the middle part of the standard zone N19 of Blow (1969) and zone MPL2 of Cita (1975) and the lower part of the *Globorotalia puncticulata*–*G. margaritae* concurrent range zone, equivalent to the middle part of the standard zone N19 of Blow (1969) and zone MPL3 of Cita (1975) (after Makled et al. 2017). Nannoplankton – zone NN12 and the lowermost part of zone NN13 (after Makled and Mandur 2016).

**Definition:** From the LO of *Impagidinium patulum* to the UO of *Selenopemphix brevispinosa*. In a single horizon in the uppermost sample 31 occurs *Impagidinium paradoxum* (Wall) Stover and Evitt, 1978.

**Samples:** 23 to 31 (depth interval 2956 to 2468 m).

**Other characteristics:** *Pentapharsodinium dalei* Indelicato and Loeblich, 1986, *Votadinium spinosum* Reid, 1977, and *Impagidinium paradoxum* are restricted to this zone. *Polykrikos schwartzii* terminates in this zone interval. The base of this zone is an unconformity (see Dino C Assemblage Zone).

#### DINO E Assemblage Zone

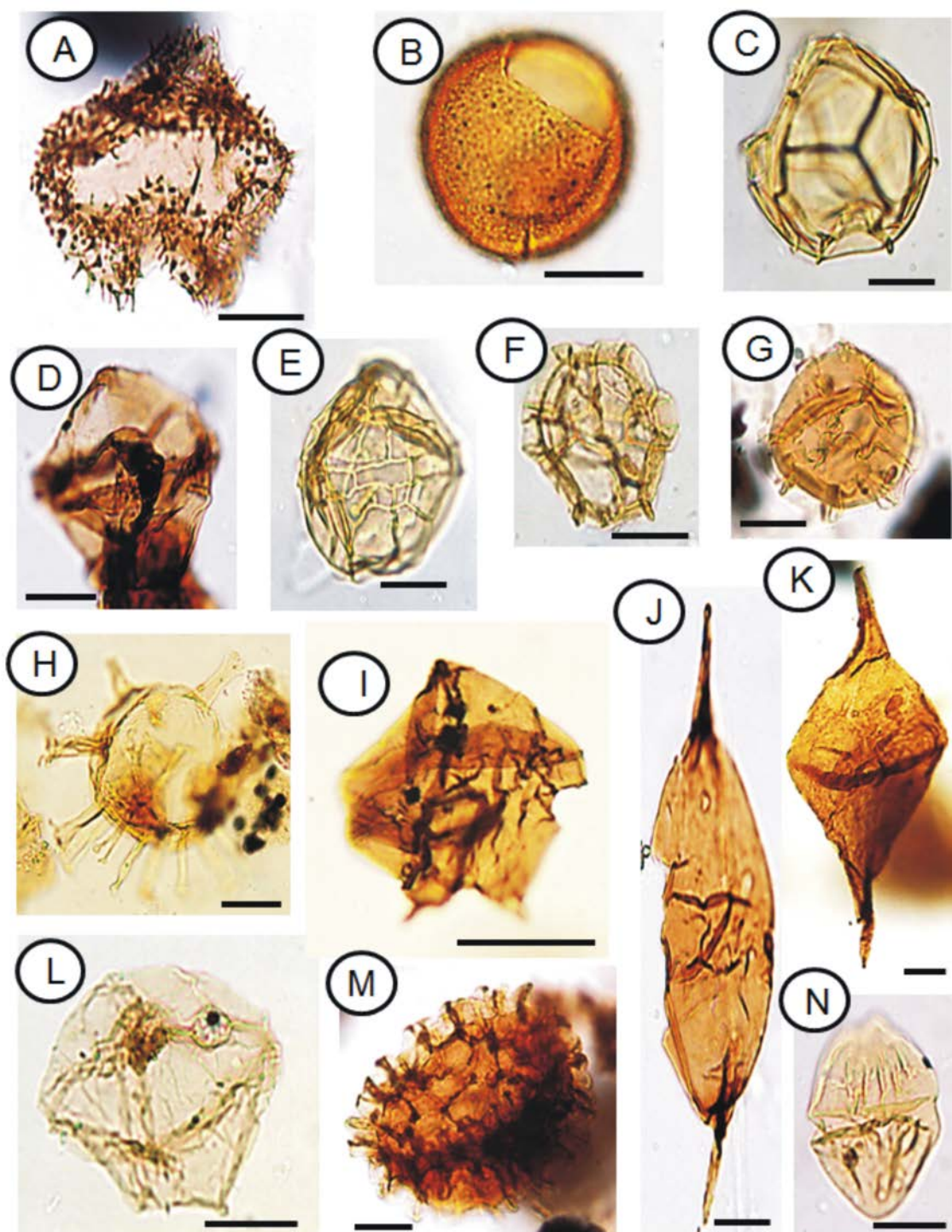
**Age:** Pliocene (Zanclean).

**Lithostratigraphic unit:** Middle Kafr El Sheikh Formation.

**Paleoenvironment:** Coastal to inner neritic (Mahmoud et al. 2024).

**Calibration:** Planktonic foraminifera – upper part of the *Globorotalia puncticulata*–*G. margaritae* Concurrent Range Zone (see above) and *Globorotalia puncticulata* Interval Zone (Makled et al. 2017), equivalent to the standard zone N19 of Blow (1969) and zone MPL4a of Cita (1975) (after Makled et al. 2017); Nannoplankton – from most of the interval of zone NN13 to zone NN15 (after Makled and Mandur 2016).

**Definition:** From above the UO of *Selenopemphix brevispinosa* and the single horizon occurrence of



Text-fig. 9. Dinoflagellate cysts in the NDO B-1 well. A – *Votadinium spinosum* Reid, 1977, b (29), 2560 m, 41.1/112. B – *Tectatodinium pellitum* Wall, 1967, b (51), 1075 m, 31.3/109. C – *Impagidinium* sp.; C – c (51), 1075 m, 51.2/97.6; E – b (12), 3102 m, 36.8/98.4. D, I, L – *Lejeuneocysta* spp.; D – b (34), 2255 m, 41.5/111.6; I – b (12), 3102 m, 36.8/98.4; L – a (14), 3090 m, 44.2/102. F – *Impagidinium paradoxum* (Wall) Stover and Evitt, 1978, d (31), 2468 m, 34.7/107.8. G – *Cymatiosphaera* sp., c (48), 1249 m, 30.7/101. H – *Homotryblium tenuispinosum* Davey and Williams, 1966, 1 (3), 3675 m, 45.6/107.6. J – *Palaeocystodinium* sp., d (9), 3340 m, 49.5/97 (reworked). K – *Andalusia* cf. *polymorpha* (Malloy) Lentini and Williams, 1977, b (12), 3102 m, 35.3/102 (reworked). M – *Polykrikos schwartzii* Bütschli, 1873, b (29), 2560 m, 33.2/109.5. N – *Dinogymnum acuminatum* Evitt, Clarke and Verdier, 1967, d (11), 3200 m, 48.3/106.9 (reworked). Slide symbols, sample numbers (in brackets), depths and microscope co-ordinates are given for every illustrated specimen. Scale bar = 20  $\mu$ m.

*Impagidinium paradoxum* to the UO of *Homotryblium* spp.

*Samples*: 32 to 37 (depth interval 2438 to 1981 m).

*Other characteristics*: *Homotryblium* spp., *Impagidinium* cf. *patulum* and *Systematophora* spp. occur in this zone. *Hystrichokolpoma rigaudiae* starts just below the top of this interval.

#### DINO F Interval Zone

*Age*: Pliocene (Piacenzian).

*Lithostratigraphic unit*: Upper Kafr El Sheikh Formation.

*Paleoenvironment*: Coastal to inner neritic to neritic (Mahmoud *et al.* 2024).

*Calibration*: Planktonic foraminifera – *Globorotalia aemiliana* Interval Zone (Makled *et al.* 2017), equivalent to the standard zone N20 of Blow (1969) and zone MPL4b–MPL5 of Cita (1975) (after Makled *et al.* 2017); Nannoplankton – zone NN16 (Makled and Mandur 2016).

*Definition*: From just above the UO of *Homotryblium* spp. to the single stratigraphic level where *Spiniferites hainanensis* Sun and Song, 1992, *Membranilarnacia*? sp. and *Hystrichosphaeridium* sp. occur. The UO of *Nematosphaeropsis labyrinthus* lies close to the top of this zone.

*Samples*: 38 to 42 (depth interval 1889 to 1706 m).

*Other characteristics*: *Achomosphaera* sp. and *Selenopemphix nephroides* terminate in this zone. This zone witnesses the lowest diversification of *Deltoidospora* spp. *Racemonocolpites* sp. and *Tricolpites* sp. terminate their occurrences in this zone interval. Within this interval, dinoflagellate cysts reach an acme representing the maximum flooding surface (Mahmoud *et al.* 2024).

#### DINO G Assemblage Zone

*Age*: Pleistocene (Gelasian–Calabrian to Ionian), see remark for Zone SPORO B.

*Lithostratigraphic unit*: Mit Ghamr Formation.

*Paleoenvironment*: Neritic (Mahmoud *et al.* 2024).

*Calibration*: The same interval as for zone SPORO B.

*Definition*: The base of this zone lies just above the single stratigraphic level where *Spiniferites hainanensis*, *Membranilarnacia*? sp. and *Hystrichosphaeridium* sp. occur. The top of the zone is uncertain.

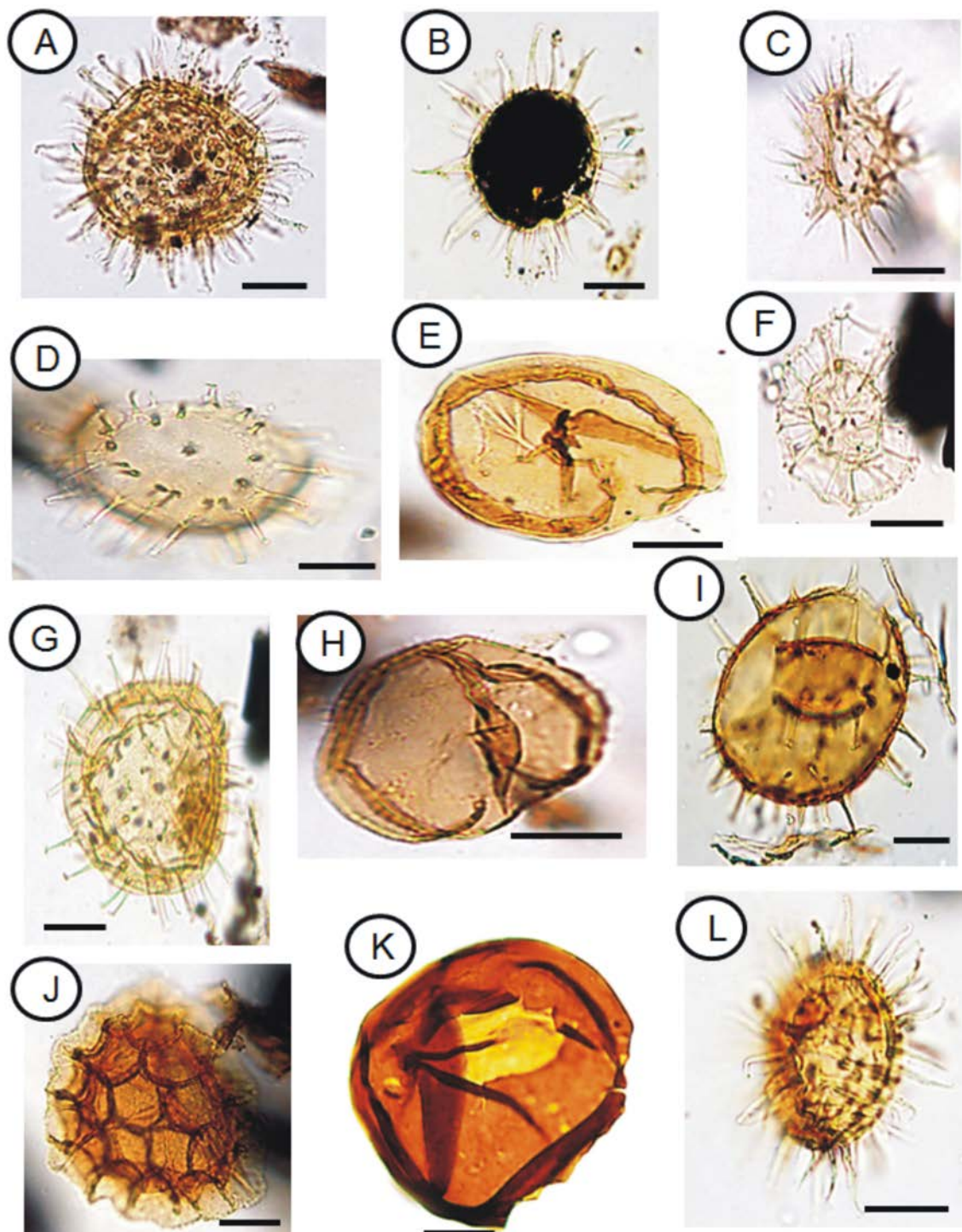
*Samples*: 44 to 53 (depth interval 1456 to 856 m).

*Other characteristics*: *Lingulodinium machaerophorum*, *Operculodinium centrocarpum*, *O. israelianum*, *Spiniferites mirabilis*, *Impagidinium patulum*, *Tectatodinium pellitum* Wall, 1967, *Hystrichokolpoma rigaudiae*, *Spiniferites* spp. and *Spiniferites* cf. *delicatus* Reid, 1974 co-occur in this zone.

#### TENTATIVE REGIONAL/INTERREGIONAL CORRELATION OF THE NDO B-1 NEogene–QUATERNARY DINOFLAGELLATES WITHIN THE MEDITERRANEAN REALM

In general, the Miocene reflects highly diversified dinoflagellate cyst assemblages in the Mediterranean and Paratethys areas, with representatives of genera such as *Spiniferites* and *Operculodinium* (e.g., Jiménez-Moreno *et al.* 2006; Popescu *et al.* 2009). In the Central Paratethys (Central Europe), the biostratigraphic zones, independently defined by foraminifera and nannofossils, correlate strongly to assemblages from the Mediterranean in the Early and Middle Miocene, a time of broad connections between both regions, which enabled floral exchange (Jiménez-Moreno *et al.* 2006). The dinoflagellate cysts of the NDO B-1 well correlate with the Upper Miocene and Pliocene sediments from the Sicilian sections, with *Lingulodinium machaerophorum* and *Operculodinium israelianum* (Londeix *et al.* 1999). However, *Impagidinium patulum* is scarce in the NDO B-1 assemblages in the Miocene–Pliocene boundary interval. The Tunisian Messinian and lower Zanclean sediments from the Jiriba-1 borehole, off Tunisia (Gulf of Hammamet) were found barren of dinoflagellate cysts, but in the upper Zanclean and Piacenzian sediments (Londeix *et al.* 1999), the dinoflagellate cysts with *Lingulodinium machaerophorum*, *Operculodinium israelianum* and *Spiniferites* spp. correlate well with the present assemblages. Popescu *et al.* (1989) analyzed rhythmic bedding in the Pliocene Trubi formation of Sicily, southern Italy. They found many dinoflagellate cyst species (e.g., *Achomosphaera* spp., *Homotryblium* spp., *Hystrichokolpoma* spp., *Impagidinium patulum*, *I. paradoxum*, *Impagidinium* spp., *Lingulodinium machaerophorum*, *Nematosphaeropsis labyrinthus*, *Polysphaeridium zoharyi*, *Spiniferites mirabilis*, *Spiniferites* spp. and *Tectatodinium pellitum*), which are closely comparable to the dinocysts association in the NDO B-1 well.

On the other hand, the hydrology of the Mediterranean area, and the amount and the source of water delivered to this basin from the Atlantic and



Text-fig. 10. Dinoflagellate cysts in the NDO B-1 well. A, B, L – *Lingulodinium machaerophorum* (Deflandre and Cookson) Wall, 1967; A – a (40), 1792 m, 44/95.4; B – t (53), 856 m, 48.7/93; L – c (51), 1075 m, 33.4/103.9. C – *Selenopemphix quanta* (Bradford) Matsuoka, 1985, c (39), 1862 m, 37.5/111.2. D – *Operculodinium israelianum* (Rossignol) Wall, 1967, c (51), 1075 m, 43.2/115.3. E – *Selenopemphix nephroides* Benedek, 1972, b (40), 1792 m, 38.5/96.9. F – *Nematosphaeropsis labyrinthus* (Ostenfeld) Reid, 1974, a (40), 1770 m, 46.1/99. G, I – *Operculodinium centrocarpum* (Deflandre and Cookson) Wall, 1967; G – a (41), 1770 m, 46.1/107.2; I – d (49), 1194 m, 30.1/103.5. H – *Selenopemphix brevispinosa* Head, Norris and Mudie, 1989b (4), 3572 m, 40.5/99.5. J – Indeterminable palynomorph, c (42), 1706 m, 42.7/95.3. K – *Brigantedinium* sp., c (23), 2956 m, 35.2/98.9. Slide symbols, sample numbers (in brackets), depths and microscope co-ordinates are given for every illustrated specimen. Scale bar = 20  $\mu$ m.

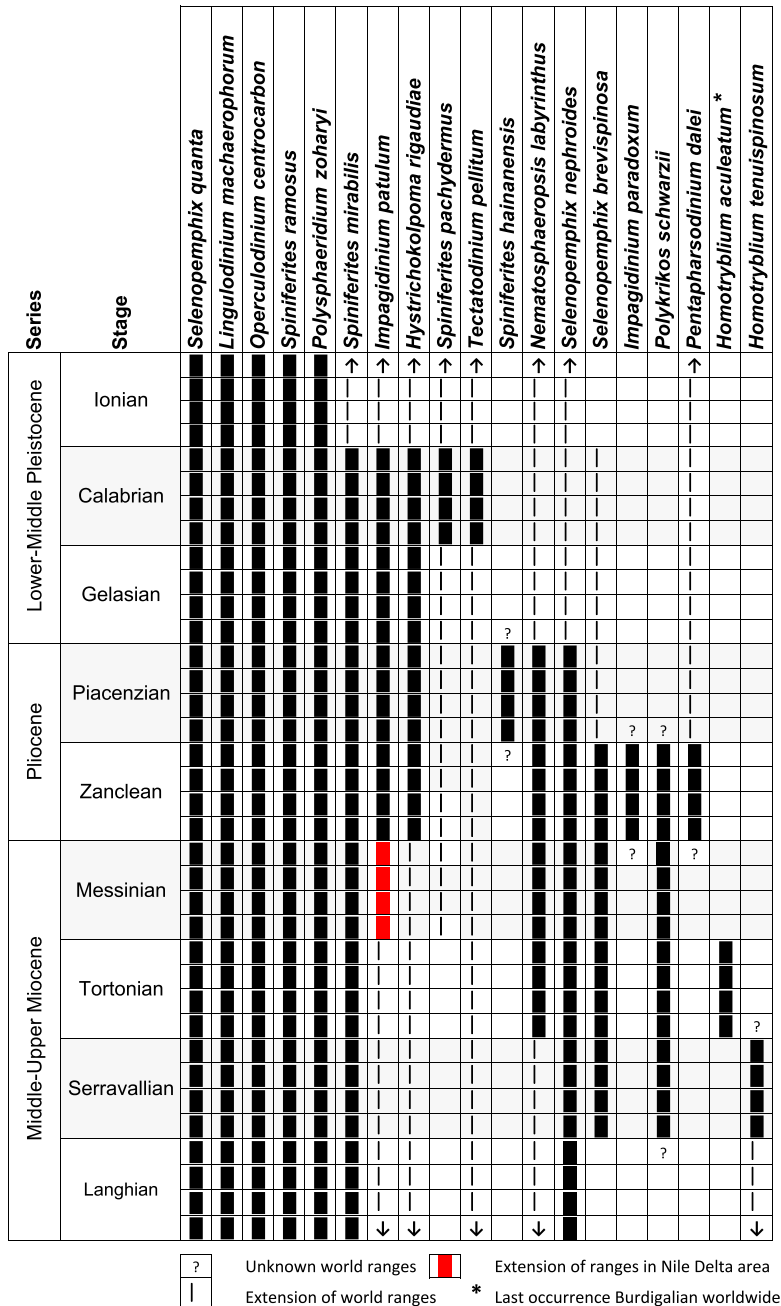
the Paratethys, in addition to the freshwater delivered from e.g., African rivers, by the end of the Miocene was controlled by orbital and tectonic drivers (see Andreetto *et al.* 2021 and references therein). Restricted marine environments were highly sensitive to climatic changes in terms of those related to gateway restriction. Significant changes in salinity, temperature, stratification and productivity appeared already before the Tortonian–Messinian boundary (Besiou *et al.* 2024). The Strait of Sicily played an important role in the process of water mass-exchange between the western and eastern Mediterranean and in the hydrodynamics of the Mediterranean (e.g., Cita and Ryan 1973). Based on these considerations, the differences that occur between the analyzed dinoflagellate cysts and other assemblages in the Mediterranean Realm can be explained. The large influence of the Nile River and the environmental restriction in the study area play a crucial role (Mahmoud *et al.* 2024). Consistently, marine stenohaline (oceanic-outer platform) dinoflagellate taxa (e.g., *Impagidinium paradoxum*, *I. patulum*, *I. striatum* (Wall) Stover and Evitt, 1978, *Nematosphaeropsis labyrinthus* and *Spiniferites mirabilis*) (Popescu *et al.* 2015) are extremely rare in the present associations. On the other hand, marine euryhaline taxa (inner platform-coastal), mainly *Homotryblium* spp., *Lingulodinium machaerophorum*, *Operculodinium centrocarpum*, *O. israelianum*, *Spiniferites ramosus* and others, in addition to marine heterotrophic taxa (inner platform-coastal) constitute the major part of the association in the well. Furthermore, taxa around the Messinian–Zanclean boundary in the present material lack brackish Paratethyan taxa [e.g., *Galeacysta etrusca* Corradini and Biffi, 1988, *Spiniferites bentorii* (Rossignol) Wall and Dale, 1970, *S. cruciformis* Wall and Dale in Wall *et al.*, 1973], which implies that influxes from the Paratethys probably did not reach the area of the NDO B-1 well (e.g., Cita and Ryan 1973). This Paratethyan impact is recorded far to the west, in the deep southwestern Mediterranean (Popescu *et al.* 2015). *Galeacysta etrusca*, first described from the uppermost Messinian of Italy (Corradini and Biffi 1988), had migrated from the Paratethys into the Mediterranean Sea during the late Messinian (see Clauzon *et al.* 2005; Popescu *et al.* 2009). The *G. etrusca* complex migrated into the Mediterranean during high sea-level connections, just before and after the peak of the Messinian Salinity Crisis (Popescu *et al.* 2009). However, two episodes of water exchange existed between the Mediterranean and the Paratethys seas during 6–5 Ma, causing a ‘Lago Mare’ biofacies along the

Mediterranean margins (Bertini *et al.* 1995; Clauzon *et al.* 2005). The absence of that taxon, along with *Spiniferites bentorii* and *S. cruciformis*, in the study area in the eastern Mediterranean, may be attributed to the disconnection and/or limited water circulation between the western and eastern Mediterranean at the Messinian–Zanclean boundary. An inverse explanation may be suggested due to the occurrence of a widespread erosion surface in the Nile Delta area (Rizzini *et al.* 1978; Metwalli *et al.* 2023; Shalaby and Sarhan 2023). This regional unconformity may account for the removal of sediments equivalent to the Lago Mare biofacies during these times.

In the regional record, the association of dinoflagellate cysts recovered from the Miocene and Pliocene sediments in the Nile Delta (El Beialy 1988) contains species in common with the NDO B-1 associations, such as *Homotryblium tenuispinosum* and *Nematosphaeropsis labyrinthus* but lacks others, such as *Lingulodinium machaerophorum*, *Operculodinium centrocarpum* and *O. israelianum*. The middle Miocene to Pliocene assemblages in the eastern Nile Delta (El Beialy 1990) have also taxa in common, such as *Spiniferites/Achomosphaera*, *Lejeuneacysta*, *Impagidinium* and *Systematophora*. The upper Miocene (as Abu Madi Formation) and lower Pliocene (Kafr El Sheikh III formation) associations, investigated by El Beialy (1992, Damanhur South-1 well, west Nile Delta) are more closely comparable to our assemblages. The middle Miocene dinoflagellate cyst association from the Shagar-1 borehole, SW Gulf of Suez, Egypt (Mahmoud 1993, dinoflagellate cysts zones A and B) contains two index taxa, i.e., *Hystrichosphaeropsis obscura* and *Cleistosphaeridium placacanthum* (as *Systematophora placacantha*) that are missing in the NDO B-1 associations. The Miocene dinoflagellate cysts recovered by Soliman *et al.* (2012, Gulf of Suez) were not recovered here, probably due to major paleoenvironmental differences between the Nile Delta and the Gulf of Suez areas. However, a synopsis of ranges was created for some selected dinoflagellate cysts in the study area (Text-fig. 11), where ranges of selected NDO B-1 dinoflagellate cysts, in terms of local Egyptian and global records, may differ.

## CONCLUSIONS

Two informal zones based on spore and pollen, and seven informal zones based on dinoflagellate cysts are suggested for the Miocene to Pliocene interval in the offshore Nile Delta area. These zones may be of regional significance, especially in the Nile



Text-fig. 11. Synopsis of ranges of selected dinoflagellate cysts identified in the studied NDO B-1 well, showing their extension in the Nile Delta area and the world.

Delta area, which was highly impacted during the Neogene by a huge river influx. This particular case reflects a characteristic palynoflora which is believed to reflect the variability in species appearance/disappearance, abundance and diversity when compared to their contemporaneous regional/interregional counterparts. The observed differences in the paly-

nofloras between the Nile Delta and adjacent areas in Miocene–Pleistocene times are most probably due to varying paleoenvironments. In a wider sense, the hydrology of the Mediterranean, the environmental and strait restriction might explain why the analyzed dinoflagellate cyst assemblages possess their own nature. Age constraints and the occurrence of a widespread

unconformity at the Messinian–Zanclean boundary in the Nile Delta area suggest either a disconnection between the eastern and western Mediterranean areas or, otherwise, a stratigraphic bias.

## Acknowledgements

The authors greatly thank the authorities of the Egyptian General Petroleum Corporation (E.G.P.C), for providing the samples and well logs for the present work. We greatly thank Przemysław Gedl (Polish Academy of Science, Kraków, Poland), an anonymous reviewer and Anna Źylińska (Editor) for their valuable comments and remarks that improved the quality of the manuscript.

## REFERENCES

Abdel Aal, A., Price, R.J., Vaitl, J.D. and Shrallow, J.A. 1994. Tectonic evolution of the Nile Delta, its impact on sedimentation and hydrocarbon potential. Egyptian General Petroleum Corporation, 12<sup>th</sup> Exploration and Production Conference, 12–15 November 1994, 19–34. EGPC; Cairo.

Abdel-Kireem, M.R., Abdou, H.F. and Samir, A.M. 1984. Pliocene biostratigraphy and palaeoclimatology of the Buseili-IX well, Nile Delta, Egypt. *Neues Jahrbuch für Geologie und Paläontologie, Monatshefte*, **10**, 577–593.

Abdou, H.F., Abdel-Kireem, M.R. and Samir, AM. 1984. Neogene planktonic foraminiferal biostratigraphy of Nile Delta. *Géologie Méditerranéenne*, **11** (2), 193–205.

Andreetto, F., Aloisi, G., Raad, F., Heida, H., Flecker, R., Agiadi, K., Lofi, J., Blondel, S., Bulian, F., Camerlenghi, A., Caruso, A., Ebner, R., Garcia-Castellanos, D., Gaullier, V., Guibourdenche, L., Gvirtzman, Z., Hoyle, T.M., Meijer, P.T., Moneron, J., Sierro, F.J., Travan, G., Tzevahirtzian, A., Vasiliev, I. and Krijgsman, W. 2021. Freshening of the Mediterranean Salt Giant: controversies and certainties around the terminal (Upper Gypsum and Lago-Mare) phases of the Messinian Salinity Crisis. *Earth-Science Reviews*, **216**, 103577.

Barber, P.M. 1981. Messinian subaerial erosion of the proto-Nile delta. *Marine Geology*, **44**, 253–272.

Benedek, P.N. 1972. Phytoplankonten aus dem Mittel- und Oberoligozän von Tönisberg (Niederrheingebiet). *Palaeontographica, Abteilung B*, **137**, 1–71.

Bertini, A., Corradini, D. and Suc, J.-P. 1995. On *Galeacysta etrusca* and the connections between the Mediterranean and the Paratethys. *Romanian Journal of Stratigraphy*, **76**, Suppl. 7, 141–142.

Besiou, E., Vasiliev, I., Kontakiotis, G., Agiadi, K., Methner, K., Andreas Mulch, A., Krijgsman, W. and Antonarakou, A. 2024. Large and rapid salinity fluctuations affected the eastern Mediterranean at the Tortonian–Messinian transition. *Palaeogeography, Palaeoclimatology, Palaeoecology*, **656**, 112568.

Blow, H.W. 1969. Late Middle Eocene to Recent planktonic foraminiferal biostratigraphy. In: Bronnimann, P. and Renz, H.H. (Eds), *Proceedings of the 1<sup>st</sup> International Conference on Planktonic Microfossils*, Geneva, 1, 199–422. E.J. Brill; Leiden.

Braman, D.R. 2001. Terrestrial Palynomorphs of the upper Santonian–?lowest Campanian Milk River Formation, southern Alberta, Canada. *Palynology*, **25**, 57–107.

Bujak, J.P., Downie, C., Eaton, G.L. and Williams, G.L. 1980. Dinoflagellate cysts and acritarchs from the Eocene of southern England. *Special Papers in Palaeontology*, **24**, 1–100.

Bütschli, O. 1873. Einiges über Infusorien. *Archiv für Mikroskopische Anatomie*, **9**, 657–678.

Cherif, O.H., El-Sheikh, H. and Mohamed, S. 1993. Planktonic foraminifera and chronostratigraphy of the Oligo-Miocene in some wells in the Isthmus of Suez and the North-Eastern reach of the Nile Delta, Egypt. *Journal of African Earth Sciences*, **16** (4), 499–511.

Cita, M.B. 1973. Pliocene biostratigraphy and chronostratigraphy. *Initial Reports of the Deep Sea Drilling Project*, **13**, 1343–1379.

Cita, M.B. and Ryan, W.B.F. 1973. The Pliocene records in deep-sea Mediterranean sediments: Time scale and general synthesis. In: Ryan, W.B.F., Hsu, K.L. et al. (Eds), *Initial Reports of the Deep Sea Drilling project, U.S. Government printing Office, Washington, D.C.*, **13** (2), 1405–1415.

Clauzon, G., Suc, J.-P., Gautier, F., Berger, A. and Loutre, M.-F. 1996. Alternate interpretation of the Messinian salinity crisis: controversy resolved? *Geology*, **24**, 363–366.

Clauzon, G., Suc, J.-P., Popescu, S.-M., Marunteanu, M., Rubino, J.-L., Marinescu, F. and Melinte, M.C. 2005. Influence of the Mediterranean sea-level changes over the Dacic Basin (Eastern Paratethys) in the Late Neogene. The Mediterranean Lago Mare facies deciphered. *Basin Research*, **17**, 437–462.

Cohen, K.M., Finney, S.C., Gibbard, P.L. and Fan, J.-X. 2013. The ICS International Chronostratigraphic Chart. *Episodes*, **36**, 199–204.

Corradini, D. and Biffi, U. 1988. Étude des dinokystes à la limite Messinien–Pliocène dans la coupe Cava Serredi, Toscane, Italie. *Bulletin des Centres de recherches exploration-production Elf-Aquitaine*, **12** (1) 221–236.

Couper, R.A. 1953. Upper Mesozoic and Cainozoic spores and pollen grains from New Zealand. *New Zealand Geological Survey Palaeontological Bulletin*, **22**, 1–77.

Davey, R.J. and Williams, G.L. 1966. The genus *Hystrichosphaeridium* and its allies. In: Davey, R.J., Downie, C., Sargeant, W.A.S. and Williams, G.L. (Eds), *Studies on Mesozoic and Cainozoic dinoflagellate cysts*. *British Museum (Natural History) Geology, Bulletin*, Supplement **3**, 53–106.

Deflandre, G. and Cookson, I.C. 1955. Fossil microplankton from Australian Late Mesozoic and Tertiary sediments. *Australian Journal of Marine and Freshwater Research*, **6** (2), 242–313.

Doyle, J.A., Jardiné, S. and Doerenkamp, A. 1982. *Afropollis*, a new genus of early angiosperm pollen, with notes on the Cretaceous palynostratigraphy and paleoenvironments of Northern Gondwana. *Bulletin des Centres de recherches exploration-production, Elf-Aquitaine*, **6**, 39–117.

Eaton, G.L., Fensome, R.A., Riding, J.B. and Williams, G.L. 2001. Re-evaluation of the status of the dinoflagellate cyst genus *Cleistosphaeridium*. *Neues Jahrbuch für Geologie und Paläontologie, Abhandlungen*, **2019** (1–2), 171–205.

E.G.P.C. (Egyptian General Petroleum Corporation), 1994. Western Desert, oil and gas fields (a comprehensive overview), 431 pp. Egyptian General Petroleum Corporation; Cairo.

Ehrenberg, C.G. 1837. Über das Massenverhältniss der jetzt lebenden Kiesel-Infusorien und über ein neues Infusorien-Conglomerat als Polirschiefer von Jastraba in Ungarn. *Abhandlungen der Königlichen Akademie der Wissenschaften zu Berlin, Physikalische Klasse*, **1836**, 109–135.

El Atfy, H., Brocke, R. and Uhl, D. 2017. Miocene palynology of the Rudeis and Kareem formations (Gharandal Group), GH 404-2A Well, Gulf of Suez, Egypt. *Abhandlungen der Senckenberg Gesellschaft für Naturforschung*, **573**, 1–134.

El Beialy, S.Y. 1988. Palynostratigraphy of Late Tertiary sediments in Kafr El Dawar well no.1, Nile delta, Egypt. *Revue de Micropaléontologie*, **30** (4), 249–260.

El Beialy, S.Y. 1990. Palynology, palaeoecology and dinoflagellate cysts stratigraphy of the Oligocene through Pliocene succession in the Qantara-1 well, eastern Nile delta, Egypt. *Journal of African Earth Sciences*, **11** (3/4), 291–307.

El Beialy, S.Y. 1992. Miocene and Pliocene Dinoflagellate cysts and other palynomorphs from the Damanhour South-1 well, western Nile delta, Egypt. *Neues Jahrbuch für Geologie und Paläontologie, Monatshefte*, **1992** (10), 577–594.

El Beialy, S.Y. 1997. Dinoflagellate cysts, sporomorphs, and other palynomorphs across the Miocene/Pliocene boundary, Kafr El Sheikh-1 well, Nile Delta, Egypt. *Neues Jahrbuch für Geologie und Paläontologie, Monatshefte*, **1997** (7), 383–398.

El Beialy, S.Y., Mahmoud, M.S. and Ali, A.S. 2005. Insights on the age, climate and depositional environments of the Rudeis and Kareem formations, GS-78-1 well, Gulf of Suez, Egypt: A palynological approach. *Revista Española de Micropaleontología*, **37** (2), 273–289.

El Hussieny, M.-A.T., Mahmoud, M.S. and Deaf, A.S. 2025. Neogene palaeoenvironments and hydrocarbon potential in the Nile Delta, Egypt: palynological evidence from an onshore well. *Palaeoworld*, **34** (5), 200966.

El-Soughier, M.I. and Mahmoud, M.S. 2019. Dinoflagellate cysts stratigraphy and paleoecology from some Lower Miocene rocks, GS9-1X well, northern Gulf of Suez, Egypt. *Journal of African Earth Sciences*, **160**, 103650.

stratigraphic framework in the Nile Delta, Egypt. *Journal of African Earth Sciences*, **9**, 89–109.

Evitt, W.R., Clarke, R.F.A. and Verdier, J.-P. 1967. Dinoflagellate studies III. *Dinogymnum acuminatum* n. gen., n. sp. (Maastrichtian) and other fossils formerly referable to *Gymnodinium* Stein. *Stanford University Publications, Geological Sciences*, **10** (4), 1–27.

Fensome, R.A., Williams, G.L., Barss, M.S., Freeman, J.M. and Hill, J.M. 1990. Acritharchs and fossil prasinophytes: an index to genera, species and infraspecific taxa. *American Association of Stratigraphic Palynologists, Contributions Series*, **25**, 1–771.

González Guzmán, A.E. 1967. A palynology study on the Upper Los Cuervos and Mirador Formations (Lower and Middle Eocene; Tibú area, Colombia), 68 pp. E.J. Brill; Leiden.

Habib, D. 1972. Dinoflagellate stratigraphy Leg 11, Deep Sea Drilling Project. In: Hollister, C.D. et al. (Eds), *Deep Sea Drilling Project, Washington, Initial Reports*, **11**, 367–425.

Hamouda, A. and El-Gharabawy, S. 2019. Impacts of neotectonics and salt diaper on the Nile fan deposit, Eastern Mediterranean. *Environmental and Earth Sciences Research Journal*, **6** (1), 8–18.

Harms, J. and Wary, J. 1990 Nile Delta. In: Said R. (Ed.), *Geology of Egypt*, 329–343. A. Balkema; Rotterdam, Brookfield.

Head, M.J., Norris, G. and Mudie, P.J. 1989a. New species of dinocysts and a new species of acritarch from the Upper Miocene and lowermost Pliocene, ODP Leg 105, Site 646, Labrador Sea. In: Srivastava, S.P. et al. (Eds), *Ocean Drilling Program, Proceedings, Scientific Results, Leg 105*, 453–466. Ocean Drilling Program; College Station, Texas.

Head, M.J., Norris, G. and Mudie, P.J. 1989b. Palynology and dinocyst stratigraphy of the Miocene in ODP Leg 105, Hole 645E, Baffin Bay. In: Srivastava, S.P. et al. (Eds), *Ocean Drilling Program, Proceedings, Scientific Results, Leg 105*, 467–514. Ocean Drilling Program; College Station, Texas.

Hsü, K.J., Ryan, W.B.F. and Cita, M. 1973. Late Miocene desiccation of the Mediterranean. *Nature*, **242**, 240–244.

Iaccarino, S. and Salvatorini, G. 1982. A framework of planktonic foraminiferal biostratigraphy for early Miocene to late Pliocene in the Mediterranean area. *Paleontology, Stratigraphy, Evolution*, **2**, 115–125.

Indelicato, S.R. and Loeblich, A.R. 1986. A revision of the marine peridinoid genera (Pyrrhophyta) utilizing hypothecal-cingular plate relationships as a taxonomic guideline. *Japanese Journal of Phycology*, **34** (3), 153–162.

Ismail, A.A., Boukhary, M. and Naby, A. 2010. Subsurface stratigraphy and micropaleontology of the Neogene rocks, Nile Delta, Egypt. *Geologia Croatica*, **63** (1), 1–26.

Jiménez-Moreno, G., Head, M.J. and Harzhauser, M. 2006. Early and Middle Miocene dinoflagellate cyst stratigraphy

of the Central Paratethys, Central Europe. *Journal of Micropalaeontology*, **25** (2), 113–139.

Lentin, J.K. and Williams, G.L. 1977. Fossil dinoflagellates: index to genera and species, 1977 edition. *Bedford Institute of Oceanography, Report Series*, **BI-R-77-8**, 1–209.

Lentin, J.K. and Williams, G.L. 1987. Status of the fossil dinoflagellate genera *Ceratiopsis* Vozzhenikova 1963 and *Cerodinium* Vozzhenikova 1963 emend. *Palynology*, **11**, 113–116.

Londeix, L., Benzakour, M., de Vernal, A., Turon, J. L. and Duc, J.-P. 1999. Late Neogene dinoflagellate cyst assemblages from the Strait of Sicile, Central Mediterranean Sea: paleoecological and biostratigraphical implications. In: Wrenn, J.H., Suc, J.-P. and Leroy, S.A.G. (Eds), *The Pliocene: Time of Change*, 65–91. American Association of Stratigraphic Palynologists Foundation; Dallas, TX.

Lourens, L.J., Hilgen, F.J., Shackleton, N.J., Laskar, J. and Wilson, D. 2004. (Appendix 2) Orbital tuning calibration and conversions for the Neogene Period. In: Gradstein, F.M., Ogg, J.G. and Smith, A.G. (Eds), *A Geologic Time Scale 2004*, 469–484. Cambridge University Press; Cambridge.

Mahmoud, M.S. 1993. Dinoflagellate cysts stratigraphy of the Middle Miocene from Shagar-1 borehole, SW Gulf of Suez, Egypt. *Newsletters on Stratigraphy*, **28** (1), 79–92.

Mahmoud, M.S., Deaf, A.S. and El Hussieny, M.-A.T. 2024. Neogene–Quaternary paleoenvironments and kerogen assessment of the NDO B-1 well, offshore Nile Delta, Egypt, Eastern Mediterranean: palynological evidence. *Acta Geologica Polonica*, **74**, e21.

Makled, W.A. and Mandur, M.M.M. 2016. Nannoplankton calendar: applications of nannoplankton biochronology in sequence stratigraphy and basin analysis in the subsurface offshore Nile Delta, Egypt. *Marine and Petroleum Geology*, **72**, 374–392.

Makled, W.A., Soliman, S.I. and Langer, M.R. 2017. Manual of Neogene foraminifera from off-shore Nile Delta (Egypt) and their biostratigraphic significance. *Marine and Petroleum Geology*, **80**, 450–491.

Mander, L., Jaramillo, C. and Oboh-Ikuenobe, F. 2023. Descriptive systematics of Upper Palaeocene–Lower Eocene pollen and spores from the northern Niger Delta, south-eastern Nigeria. *Palynology*, **47**, 1–59.

Mandur, M.M.M. and Makled, W.A. 2016. Implications of calcareous nannoplankton biostratigraphy and biochronology of the Middle–Late Miocene of the Nile Delta, Egypt. *Arabian Journal of Geosciences*, **9** (203), 1–17.

Mantell, G.A. 1854. *The Medals of Creation; or, First Lessons in Geology and the Study of Organic Remains*; Second Edition, 930 pp. Henry G. Bohn; London.

Matsuoka, K. 1985. Organic-walled dinoflagellate cysts from surface sediments of Nagasaki Bay and Senzaki Bay, west Japan. *Faculty of Liberal Arts, Nagasaki University, Natural Science, Bulletin*, **25** (2), 21–115.

Metwalli, F.I., Ismail, A., Metwally, M.S. and El Shafei, I.M. 2023. Sequence stratigraphic evaluation for the Abu Madi Formation, Abu Madi/El Qar'a/Khilala gas fields, onshore Nile Delta, Egypt. *Petroleum Research*, **8**, 514–523.

Müller, J. 1968. Palynology of the Pedawan and Plateau Sandstone Formation (Cretaceous–Eocene) in Sarawak, Malaysia. *Micropalaeontology*, **14**, 1–37.

Nakoman, E. 1966. Contribution à l'étude palynologique des formations tertiaires du Bassin de Thrace. *Annales de la Société Géologique Du Nord*, **46**, 65–107.

N.C.G.S. (National Committee of Geological Sciences) 1976. Miocene rock stratigraphy of Egypt. *Egyptian Journal of Geology*, **18**, 1–69.

Ouda, Kh. and Obaidalla, N. 1995. The geologic evolution of the Nile Delta area during the Oligocene–Miocene. *Egyptian Journal of Geology*, **39**, 77–111.

Popescu, S.-M., Dalesme, F., Jouannic, G., Escarguel, G., Head, M.J., Melinte-Dobrinescu, M.C., Suto-Szentai, M., Bakrac, K., Clauzon, G. and Suc, J.-P. 2009. *Galeacysta etrusca* complex: dinoflagellate cyst marker of Paratethyan influxes to the Mediterranean Sea before and after the peak of the Messinian Salinity Crises. *Palynology*, **33** (2), 105–134.

Popescu, S.-M., Dalibard, M., Suc, J.-P., Barhoun, N., Melinte-Dobrinescu, M.-C., Bassetti, M.A., Deaconu, F., Head, M.J., Gorini, C., Do Couto, D., Rubino, J.-L., Auxietre, J.-L. and Floodpage, J. 2015. Lago Mare episodes around the Messinian–Zanclean boundary in the deep southwestern Mediterranean. *Marine and Petroleum Geology*, **66**, 55–70.

Price, A.M. and Pospelova, V. 2014. *Spiniferites multisphaerus*, a new dinoflagellate cyst from the Late Quaternary of the Guaymas Basin, Gulf of California, Mexico. *Palynology*, **38**, 101–116.

Reid, P.C. 1974. Gonyaulacacean dinoflagellate cysts from the British Isles. *Nova Hedwigia*, **25**, 579–637.

Reid, P.C. 1977. Peridiniacean and glenodiniacean dinoflagellate cysts from the British Isles. *Nova Hedwigia*, **29**, 429–463.

Rizzini, A., Vessani, F., Cococetta, V. and Milad, G. 1978. Stratigraphy and Sedimentation of Neogene–Quaternary section in the Nile Delta area. *Marine Geology*, **27**, 327–348.

Roveri, M., Bertini, A., Cosentino, D., Di Stefano, A., Gennari, R., Gliozzi, E., Grossi, F., Iaccarino, S.M., Lugli, S., Manzi, V. and Taviani, M. 2008. A high-resolution stratigraphic framework for the latest Messinian events in the Mediterranean area. *Stratigraphy*, **5** (3–4), 327–345.

Sah, S.C.D. 1967. Palynology of an Upper Neogene profile from Rusizi Valley (Burundi). *Annales Musée Royal de l'Afrique Centrale*, **8**, 1–173.

Sarjeant, W.A.S. 1970. The genus *Spiniferites* Mantell, 1850 (Dinophyceae). *Grana*, **10**, 74–78.

Sestini, G. 1989. Nile Delta: a review of depositional environments and geological history. In: Whateley, M.K.G. and Pickering, K.T. (Eds), *Deltas: Sites and Traps for Fossil*

Fuel. *Geological Society of London Special Publications*, **41**, 99–127.

Sestini, G. 1995. Egypt. In: Kulke, H. (Ed.), *Regional Petroleum Geology of the World, Part II: Africa, America, Australia and Antarctica*. Beiträge zur regionalen Geologie der Erde, Bd. 21–22, 57–87. Bornträger; Stuttgart.

Shalaby, A. and Sarhan, M.A. 2023. Pre- and post-Messinian deformational styles along the northern Nile Delta Basin in the framework of the Eastern Mediterranean tectonic evolution. *Marine Geophysical Research*, **44**, 22.

Singh, C. 1983. Cenomanian microfloras of the Peace River area, northwestern Alberta. *Research Council of Alberta Bulletin*, **44**, 1–322.

Soliman, A., Coric, S., Head, M.J., Pillar, W.E. and El Beialy, S.Y. 2012. Lower and Middle Miocene biostratigraphy, Gulf of Suez, Egypt based on dinoflagellate cysts and calcareous nannofossils. *Palynology*, **36**, 38–79.

Stover, L.E. and Evitt, W.R. 1978. Analyses of pre-Pleistocene organic-walled dinoflagellates. *Stanford University Publications, Geological Sciences*, **15**, 1–300.

Sun, X. and Song, Z. 1992: Quaternary dinoflagellates from arenaceous dolomite in Hainan Island. *Acta Micropalaeontologica Sinica*, **9** (1), 45–52.

Traverse, A. 2007. *Paleopalynology*, 813 pp. Springer; Dordrecht, The Netherlands.

Wall, D. 1967. Fossil microplankton in deep-sea cores from the Caribbean Sea. *Palaeontology*, **10** (1), 95–123.

Wall, D. and Dale, B. 1970. Living hystrichosphaerid dinoflagellate spores from Bermuda and Puerto Rico. *Micropaleontology*, **16**, 47–58.

Wall, D., Dale, B. and Harada, K. 1973. Descriptions of new fossil dinoflagellates from the Late Quaternary of the Black Sea. *Micropaleontology*, **19**, 18–31.

Verteul, L. de and Norris, G. 1992. Miocene protoperidiniancean dinoflagellate cysts from the Maryland and Virginia coastal plain. In: Head, M.J. and Wrenn, J.H. (Eds), *Neogene and Quaternary dinoflagellate cysts and acritarchs*, 391–430. American Association of Stratigraphic Palynologists; College Station, TX.

Verteul, L. de and Norris, G. 1996. Miocene dinoflagellate stratigraphy and systematics of Maryland and Virginia. *Micropaleontology*, **42**, Supplement, 1–172.

Zhao, Y. and Morzadec-Kerfourn, M.-T. 1994. Nouveaux kystes de dinoflagellés: *Spiniferites pacificus* nov. sp. et *Pentadinium netangei* nov. sp. de Pléistocène du nord-ouest Pacifique. *Geobios*, **27** (3), 261–269.

Manuscript submitted: 30<sup>th</sup> May 2025

Revised version accepted: 24<sup>th</sup> September 2025

Numerical counts of the palynomorphs recovered from the NDO B-1 well.

Sample no.	Depth (ft)	Depth (m)	SPORES		POLLEN		TOTAL SPORES AND POLLEN		FRESHWATER ALGAE		TOTAL TERRESTRIAL PALYNOmorphs		TOTAL DINOFAGELLATE CYSTS		TOTAL MARINE PALYNOmorphs		TOTAL PALYNOmorphs		REWORED PALYNOmorphs		
			Spores	Spores	Pollen	Pollen	Total	Total	Oocystis parvus	Oocystis/Scincozoopte spp.	Total	Total	Total	Total	Total	Total	Total	Total	Total	Total	
53	2810	856	Lyngbyospores sp.								1	111	3	212	62	2	64	276			
52	3380	1030	Roussispores sp.								2	81	2	202	60	0	60	262			
51	3530	1075	Foveospores spp. (sensu lato)								4	115	2	396	56	1	57	455			
49	3920	1194	Brettsporites sp.								3	73	1	184	38	1	39	223			
48	4100	1249	Polydactylospores spp.								3	33	4	1	1	1	1	184			
47	4220	1286									2	26	1	1	2	30		1			
46	4500	1371									6	6	50	7	2	10	29	1			
45	4700	1432									5	5	15	1	10	5	25				
44	4780	1456									2	4	16	5	1	6	25				
42	5600	1706									1	4	4	8	8	27	1				
41	5810	1770									1	1	3	8	9	31					
40	5880	1792									1	2	12	4	15						
39	6110	1862									1	1	12	47							
38	6200	1889									3	8	7	3	37						
37	6500	1981									3	1	2	4	3	14					
36	7000	2133									3	3	10	1	4	35					
35	7200	2194									3	1	10	4	31	1					
34	7400	2255									1	1	2	8	2	20					
32	8000	2438									1	1	1	1	15						
31	8100	2468									2	1	3	2	9						
30	8200	2499									2	1	4	4							
29	8400	2560									3	2	2	2	11						
28	8500	2590									4	3	2	3	7	32					
X	3	13									X	1	1	42							
26	9200	2804									4	1	3	2	5	13					
25	9580	2919									4	1	8	4	2						
24	9600	2926									4	2	8	5	38						
23	9700	2956									6	1	30	5	9	3	2	3			
21	9960	3035									3	2	1	2	1	8					
20	9980	3041									1	1	3	7	21						
19	10000	3048									1	2	1	9	10	30					
18	10060	3066									2	2									
16	10100	3078									2	3	18	2	4	1	4	2			
15	10120	3084									2	3	5	5	4	17	3	10	7	3	
14	10140	3090									3	1	4	4	9	1	4	1	9		
13	10160	3096									1	1	2	1	9	15					
12	10180	3102									2	4	2	10	5	26					
11	10500	3200									1	1	3	8	10	7	23	5	8	3	
10	10820	3297									2	2	1	2	6	20					
9	10960	3340									2	6	17	24	7	5	4	2	1		
7	11260	3432									2	1	1	5	5	5	2	1	1		
5	11620	3541									2	5	7	2	4	2	1	5	1		
4	11720	3572									1	3	8	6	4	6	2	6	3		
3	12060	3675									1	1	6	1	1	1	1	4	2		
2	12400	3779									1	1	1	1	1	1	2	1	1		
1	12460	3797									1	1	8	4	4	1	1	1	2	1	

X

Qualitative findings